All-electron, linear response theory of local environment effects in magnetic, metallic alloys and multilayers

1995 J. Phys.: Condens. Matter 7 1863

(http://iopscience.iop.org/0953-8984/7/9/012)

J. Phys.: Condens. Matter 7 (1995) 1863–1887. Printed in the UK

All-electron, linear response theory of local environment effects in magnetic, metallic alloys and multilayers

M F Ling†, J B Staunton† and D D Johnson‡

† Department of Physics, University of Warwick, Coventry, UK

‡ Computational Materials Science Department, Sandia National Laboratories, Livermore, CA, USA

Received 26 October 1994

Abstract. We present a theoretical framework for describing atomic short-range order and its effect upon such quantities as magnetization and hyperfine fields in magnetic alloys. All electronic effects are accurately described from a 'first-principles', density functional formalism, within the restriction of a rigid, uniform lattice. These effects include the filling of the spin polarized electronic states, Fermi surface contributions, and the rearrangement of charge and changes to the magnetization as the chemical composition of the alloy fluctuates. We have calculated the magnetochemical response for bulk $Fe_{87}V_{13}$ and $Cr_{70}Fe_{30}$ magnetic alloys to compare to those obtained from spin polarized neutron scattering experiments. We also show the utility of these response functions for investigating the changes in, for example, the moments and hyperfine fields for multilayers with varying textures in the case of FeV.

1. Introduction

A challenging problem to study in metal alloys is the subtle interplay between compositional and magnetic interactions and the dependence of the magnetic properties on the local chemical environment. In these systems, magnetism is connected to the overall compositional ordering, as well as the local chemical environment, in a subtle and complicated way. For example, chemically ordered Ni-Pt is anti-ferromagnetic but its chemically disordered counterpart is ferromagnetic [1]. A close link between magnetic and compositional ordering is displayed in nickel rich Ni–Fe alloys. $Ni_{75}Fe_{25}$ is paramagnetic at high temperatures, it becomes ferromagnetic at about 900 K and then, when just 100 K cooler, it chemically orders into the Ni_3Fe $L1_2$ phase [2]. Similarly, with the advent of modern deposition techniques, artificial materials, such as compositionally modulated systems (CMS), also exhibit varied environmentally dependent properties, especially near interfacial regions [3, 4, 5, 6].

Such physical effects are very important to materials design and can be investigated by a variety of experimental techniques. Neutron or x-ray scattering experiments provide information regarding atomic short-range order, mean magnitude of local moments or lattice parameters, for example, while methods such as Mössbauer spectroscopy and nuclear magnetic resonance, which probe each atomic position separately, provide information, say, on changes of moments, isomer shifts and hyperfine fields due to local environment effects, such as atomic short-range order or clustering.

It has long been recognized that electronic structure plays a crucial role in determining the states of compositional and magnetic order in metallic alloys. It is important then to

0953-8984/95/091863+25$19.50

obtain a microscopic understanding of what gives rise to the effects and, equally, to predict the variety of behaviours that might occur. A quantitative understanding of the electronic mechanisms that cause the ordering is therefore important for the design of alloys with particular new physical properties. It follows that it is necessary to describe the many-electron system as accurately as possible when trying to determine the various correlations and local environmental effects in the alloys.

From a theoretical point of view, the study of the electronic structure of alloys from a parameter free approach is of special importance since this allows us to describe not only the inherent atomic and magnetic correlations on an equal footing but also the electronic effects, or so-called driving mechanisms, responsible for the observed behaviour. Over the past decade or so significant progress has been made in this area. An *ab initio* description of metallic alloys based on the self-consistent field, Korringa–Kohn–Rostoker coherent potential approximation (SCF–KKR–CPA) formalism developed by some of us and other coworkers [2] has proved to be very successful in providing a starting point for a study of the atomic and magnetic correlations in a variety of metallic alloys. Recently, this mean field type theory has been extended and now it treats all electronic effects such as band filling, electrostatics ('charge transfer') and exchange–correlation effects on an equal footing [7, 8], within the constraint that the underlying lattice is rigidly fixed.

One of the problems of treating magnetism at finite temperatures in metals is finding an appropriate description of the magnetic interactions. On the one hand, there is a Stoner type, effective one-electron description of ferromagnetism suitable for metals; on the other, a picture of fluctuating 'local moments' historically more pertinent to magnetic insulators. One possible merger of these two pictures is provided by the so-called disordered local moments (DLM) theory which describes electrons moving through effective magnetic fields characterizing local moments associated with lattice sites and which are set up by all the other electrons. This approach has been reasonably successful in describing the magnetic correlations in the paramagnetic state of metals and alloys [10, 11, 12, 9]. It has recently been used as a basis for a theory of atomic pair correlations in the compositionally disordered states of these systems [9]. Such a theory can deal with the paramagnetic regime of a compositionally disordered alloy which has a magnetically ordered ground state and can determine whether or not the compositional ordering transition temperature T_c^{comp} is higher than any magnetic ordering temperature T_c^{mag}.

For situations where $T_c^{comp} < T_c^{mag}$, magnetic structure can have a profound effect upon the compositional ordering tendencies. As such, a 'first-principles' theory of compositional ordering in magnetic systems must include the effects arising from a spin polarized electronic structure. We can then study the effects of exchange splitting the electronic states on chemical ordering tendencies, as specified in wave-vector space by the compositional pair correlation function $\alpha(q)$ (or the Warren–Cowley short-range order parameter), which is accessible from diffuse scattering experiments. A theoretical formalism for dealing with compositional correlations in magnetic alloys in which some of these electronic effects were included was developed by Staunton *et al* [2]. Our present work is an extension so that all the aforementioned electronic effects, in particular magnetism, are fully incorporated, and this mean field theory is further improved by the inclusion of Onsager cavity fields [13, 14] to maintain sum rules not traditionally obeyed in mean field approaches. It is thus the generalization to ferromagnetic alloys of the work contained in [7, 8] which was applicable to non-magnetic alloys.

Based on the same spin polarized electronic structure calculation, we will focus particularly on the local environmental effects on magnetizations using our magnetocompositional pair correlation function, $\Upsilon(q)$. It is one of those quantities, resulting

from the underlying electronic structure of the disordered state, that can be deduced from spin polarized neutron scattering experiments [15]. The diffuse scattering of polarized neutrons from a magnetic binary alloy is a result of three processes: nuclear scattering, magnetic scattering and the spin dependent nuclear–nuclear scattering. For neutrons polarized (anti-) parallel, $\epsilon = (-) + 1$ to the magnetization, the cross-section per atom may be written [16] as:

$$(\mathrm{d}\sigma/\mathrm{d}\Omega)^{\epsilon} = \mathrm{d}\sigma^{NN}/\mathrm{d}\Omega + \epsilon(\mathrm{d}\sigma^{NM}/\mathrm{d}\Omega) + \mathrm{d}\sigma^{MM}/\mathrm{d}\Omega. \tag{1}$$

Neglecting the difference in the experimental form factors of each alloy species, it can be shown that the first and third terms in equation (1) are proportional to the Warren–Cowley short-range order parameter $\alpha(q)$ and the longitudinal magnetic susceptibility $\chi(q)$, respectively. $\chi(q)$ is also available from within our formalism [1]. The interference term arising from the effects of cross-correlation (i.e., the magnetocompositional correlation, $\Upsilon(q)$) may be extracted by measuring the scattering from both polarizations, i.e.

$$\Delta\mathrm{d}\sigma/\mathrm{d}\Omega = 2\,\mathrm{d}\sigma^{NM}/\mathrm{d}\Omega. \tag{2}$$

As we shall show analytically within our approach $\Upsilon(q)$ can be separated into a product of correlation and response functions; namely, $\Upsilon(q)$ is found to be $\alpha(q)\gamma(q)$, where $\gamma(q)$ is what we refer to as a moment–chemical response and will be discussed in detail.

Through the technique of isotope substitution or null matrix scattering, both $\alpha(q)$ and $\chi(q)$ can be separated from the sum of polarized cross-section measurements [15]. Then $\gamma(q)$ may be deduced indirectly, i.e. the dependence of the moment on the chemical environment may be extracted. Notably, by considering a linear superposition of perturbations and phenomenological parameters, Marshall [17] gives formulae of the same form for the scattering cross-section as the equations we derive to describe chemical environment effects. Extensions of this approach have been developed by Medina and Cable [16] and Hicks [18] to explain both the chemical and magnetic environment effects which are reflected in polarized neutron scattering experiments. Within our parameter free theory, various local quantities may be directly compared to experiment and to the available phenomenological models to give further insight into these environmental effects.

In the next section, we present a brief review of the basic formalism and a derivation will be given for the compositional correlation function, $\alpha(q)$. This quantity measures the alloy's tendency to order compositionally, or phase segregate, as temperature is lowered and can be directly compared with diffuse nuclear neutron (or electron and x-ray) scattering data. In section 3, we show the origin of the magnetocompositional pair correlation function, $\Upsilon(q)$ (or more importantly for this work $\gamma(q)$), which provides a measure of the magnetic moments' dependence on the local compositional environment and can be compared with polarized neutron measurements. We keep the details of the derivation brief since full accounts of the approach for paramagnetic alloys has been published elsewhere [7, 8, 9, 19, 20]. We emphasize instead the places where the attributes of the ferromagnetic system come into play. In the penultimate section we describe our calculations of the magnetocompositional correlation functions for bulk $Cr_{70}Fe_{30}$ and $Fe_{87}V_{13}$ alloys. Where available we compare these to experimental data. We also use our results to explore in a perturbative fashion the magnetic structures of some Fe/V multilayers and modulated alloys. The final section makes some concluding remarks.

2. Compositional ordering in magnetic alloys

To put the discussion and derivation of the response functions on a clearer footing, we begin with a brief overview of a 'first-principles' treatment of the electronic structure

of a ferromagnetic alloy, A_cB_{1-c}, in the compositionally disordered state within the self-consistent field, Korringa–Kohn–Rostoker, coherent potential approximation (SCF–KKR–CPA) formalism [21, 22]. Calculations of the electronic and magnetic structure and total energy of random alloys based on the KKR–CPA formalism are quite commonplace now. We will base our approach for a linear response investigation of fluctuations in chemical and magnetic properties within chemically random alloys on this foundation.

For finite temperatures, one must use the formalism of finite-temperature density functional theory. Within the present context of the KKR–CPA, this has been discussed in detail by Johnson *et al* [22] for electronic total energies (or grand potentials), and for response theory by Staunton *et al* [1]. Consider a many-electron system in an external potential $V^{\text{ext}} = \sum_i v_i^{\text{ext}}(r_i)$ set up by the nuclei in a crystal lattice and external magnetic field $B^{\text{ext}} = \sum_i b_i^{\text{ext}}(r_i)$, where $r_i = r - R_i$, R_i denoting the position of a lattice site. It can be shown that in the grand canonical ensemble, at a given temperature T and chemical potential ν, the equilibrium charge $\rho(r)$ and magnetization $m(r)$ densities are determined by the external potential and magnetic field. The correct equilibrium charge and magnetization densities are obtained by minimizing the Gibbs grand potential Ω via the variational principle. Staunton *et al* [1] has shown via the variational spin density functional theory that the appropriate electronic grand potential can be written as

$$\Omega = \int \mathrm{d}\epsilon\, f(\epsilon - \nu)\epsilon n(\epsilon) - \frac{1}{2}\int\int \mathrm{d}r\,\mathrm{d}r'\,\frac{\rho(r)\rho(r')}{|r-r'|} + \Omega_{\text{xc}} - \int \mathrm{d}r\left(\frac{\delta\Omega_{\text{xc}}}{\delta\rho(r)}\rho(r) + \frac{\delta\Omega_{\text{xc}}}{\delta m(r)}\cdot m(r)\right). \tag{3}$$

Ω_{xc} is the exchange and correlation contribution to the Gibbs free energy. Here the effective single-particle Green function, $\tilde{G}$, defines everything within the formalism. For example, the single-particle density of states is given by

$$n(\epsilon) = -\frac{1}{\pi}\mathrm{Im}\int \mathrm{d}r\,\mathrm{Tr}\left[\tilde{G}(r, r; \epsilon)\right]. \tag{4}$$

We note that $\tilde{G}$ is determined from a system of non-interacting electrons moving within an effective potential $\tilde{W}^{\text{eff}}$, i.e.,

$$\tilde{W}^{\text{eff}} = V^{\text{ext}}\tilde{\mathbf{1}} - B^{\text{ext}}\cdot\sigma + e^2\tilde{\mathbf{1}}\int \mathrm{d}r'\frac{\rho(r')}{|r-r'|} + \tilde{\mathbf{1}}\frac{\delta\Omega_{\text{xc}}}{\delta\rho(r)} + \frac{\delta\Omega_{\text{xc}}}{\delta m(r)}\cdot\sigma. \tag{5}$$

It satisfies the following set of equations

$$\left[\left(\epsilon + (\hbar^2/2m)\nabla^2\right)\mathbf{1} - \tilde{W}^{\text{eff}}\right]\tilde{G}(r, r'; \epsilon) = \tilde{\mathbf{1}}\delta(r - r') \tag{6}$$

$$\rho(r) = -\frac{1}{\pi}\mathrm{Im}\int \mathrm{d}\epsilon\, f(\epsilon - \nu)\mathrm{Tr}\left[\tilde{G}(r, r; \epsilon)\right] \tag{7}$$

$$m(r) = -\frac{1}{\pi}\mathrm{Im}\int \mathrm{d}\epsilon\, f(\epsilon - \nu)\mathrm{Tr}\left[\sigma\cdot\tilde{G}(r, r; \epsilon)\right] \tag{8}$$

where $\tilde{\mathbf{1}}$ is a 2×2 unit matrix and σ is the Pauli spin matrices.

The equations (6), (7) and (8) illustrate the spin polarized, self-consistent, band structure basis to the many-electron phenomenon, which, in the limit of pure metals, produces the picture of rigidly exchange split bands found in the traditional Stoner theory of metallic magnetism [23]. It is usual to make the local approximation for Ω_{xc} [24]. Stocks and Winter [21] and Johnson *et al* [22, 25] have discussed in detail how this formalism may be applied to randomly disordered, paramagnetic and ferromagnetic alloys A_cB_{1-c}. A tractable scheme for calculating the electronic structure of an alloy of concentration c

can be found in the mean field approach of the CPA. This is achieved by minimizing the configurationally averaged Gibbs grand potential with respect to the partially averaged charge and magnetization densities, $\langle\rho\rangle_{t\mathrm{A(B)}}$ and $\langle\mu\rangle_{t\mathrm{A(B)}}$. The CPA is used to construct an effective medium. The motion of an electron through this medium approximates, on average, its motion through the compositionally disordered alloy. Again, details of the calculation of the electronic structure via the KKR–CPA scheme can be found elsewhere [22].

Next, we turn our attention to the compositional ordering in an alloy which has been successfully described in terms of concentration waves [26, 27]. This method is a general framework (independent of the spatial extent of the effective interactions) for describing any compositional inhomogeneity, for instance, within an alloy in terms of a Fourier expansion, where the wave-vector specifies the type of ordering (or clustering). For example, a Cu_3Au type (or $L1_2$ type) ordered alloy can be described by concentration waves with wave-vectors $\boldsymbol{q} = (1, 0, 0)$, whereas a phase-segregating alloy is signified by the $\boldsymbol{q} = (0, 0, 0)$ wave-vector. We only require a convenient set of thermodynamic variables with which to work. Thus, any configuration of an alloy can be defined in terms of site occupation variables, $\{\xi_i\}$, where ξ_i is unity (zero) if the atom occupying lattice site i is A (B). With $\langle\ldots\rangle$ referring to the thermodynamic average, the concentration at site j, c_j, is $\langle\xi_j\rangle$, and represents the likelihood of an A atom occupying site j. The compositional pair correlation function α_{jk} is then given by $\alpha_{jk} = \beta(\langle\xi_j\xi_k\rangle - \langle\xi_j\rangle\langle\xi_k\rangle)$, where $\beta = (k_{\mathrm{B}}T)^{-1}$. This is but one quantity that is accessible through diffuse scattering experiments and that we can calculate from linear response about the KKR–CPA solutions in the high-temperature, disordered alloy. In this regard, it is a first-principles version of the concentration wave method developed by Khachaturyan [27]. (Within the first-principles approach, this theory has been generalized to an N-component case, with $N > 2$, for chemical short-range order only [28].)

The approach necessary to proceed is similar to that for paramagnetic alloys elaborated by Staunton, Johnson and Pinski [7, 8] in which the electronic structure (band filling), charge rearrangement ('charge transfer') and exchange–correlation effects are all treated on equal footing. The essential difference is, of course, the spin polarized electronic structure of the alloy. Exchange splitting of the electronic states plays an important role from the outset. As such, it is not a trivial generalization of that previous work.

We begin by writing down formally the grand potential for a system of electrons in a particular configuration of nuclei using the SDF theory, i.e., $\Omega\{\xi_i\}$. At a given temperature T, by averaging over the compositional fluctuations with measure

$$P\{\xi_i\} = \exp(-\beta\Omega\{\xi_i\}) \Big/ \prod_i \sum_{\xi_i=0,1} \exp(-\beta\Omega\{\xi_i\}) \tag{9}$$

and by using the Feynman–Peierls Inequality [29], the probability of finding an A atom on a particular site i is

$$c_i = \frac{1}{1 + \exp(\beta[\langle\Omega\{\xi_j\}\rangle_{\xi_i=1} - \langle\Omega\{\xi_j\}\rangle_{\xi_i=0}])}. \tag{10}$$

Here $\langle\Omega\{\xi_j\}\rangle_{\xi_i=1(0)}$ is the average of the (inhomogeneous) grand potential over all configurations but with the occupation on the ith site fixed at $\xi_i = 1$ (0), either A or B, respectively. Such averages are readily available from the SCF–KKR–CPA framework [7]. Note that, in principle, the probability of occupation can vary from site to site but it is only the case of a homogeneous probability distribution, $c_i = c$, that can be tackled in practice with the KKR–CPA method.

Using response theory and the fluctuation dissipation theorem, it is however possible to write down and calculate the various correlation functions appropriate to the system. Firstly, we will consider the response of the homogeneous system to the application of an

inhomogeneous external chemical potential, which couples to the occupation variables $\{\xi_i\}$, such that a term

$$\sum_i (v_i - \eta)\xi_i = \sum_i v_i \xi_i \tag{11}$$

is added to the grand potential $\Omega\{\xi_i\}$. (η is the chemical potential difference such that the number of A and B sites remains constant.) This additional potential, different on every site, induces a change in the probabilities of occupation on every site $\{\delta c_i\}$. This induced change on the ith site is written via (10) (to lowest order in the applied field about the homogeneous CPA) as

$$\delta c_i \simeq -\beta c(1-c)(\langle \delta\Omega \rangle_{i\mathrm{A}} - \langle \delta\Omega \rangle_{i\mathrm{B}}). \tag{12}$$

Of crucial importance for some of the later discussion in this paper, it also causes changes to the moments from site to site $\{\delta\mu_i^{\mathrm{A(B)}}(r_i)\}$ as well as rearranging the charge $\{\delta\rho_i^{\mathrm{A(B)}}(r_i)\}$. All three types of fluctuation are intimately connected, where the latter two are typically neglected in other models.

The details of extracting expressions for the correlation functions from the underlying electronic structure are given in previous publications [7, 8]. However, we note that in order to solve the resulting highly coupled equations [7], we make two simplifying assumptions. Firstly, we assume that $\delta\mu_i^{\mathrm{A(B)}}(r_i) = \delta\mu_i^{\mathrm{A(B)}} f^{\mathrm{A(B)}}(r_i)$ where $\int \mathrm{d}r_i\, f^{\mathrm{A(B)}}(r_i) = 1$. We have numerically verified this form for a limited set of cases. Secondly, we choose (for reasons discussed in [7]) to expand the charge fluctuations in terms of a basis set, i.e. $\delta\rho_i^{\mathrm{A(B)}}(r_i) = \sum_{n=1}^{3} \rho_i^{\mathrm{A(B)},n} f_n(r_i)$. The functions $f_n(r_i)$ are chosen as even Legendre polynomials [7], which satisfy the normalization $u_1\delta_{nm} = \int \mathrm{d}r_i\; f_n(r_i) f_m(r_i)$ with u_1 a constant. It is possible to formulate a theory of these interdependent fluctuations through the formal framework of an inhomogeneous CPA.

As noted above, the compositional, charge and magnetic responses to application of inhomogeneous chemical fields, i.e.,

$$\alpha_{ij} = \frac{\delta c_i}{\delta v_j} \tag{13}$$

$$\rho^n_{ij,\,\mathrm{A(B)}} = \frac{\delta\rho_i^{\mathrm{A(B)},n}}{\delta v_j} \tag{14}$$

$$\mu_{ij,\,\mathrm{A(B)}} = \frac{\delta\mu_i^{\mathrm{A(B)}}}{\delta v_j} \tag{15}$$

are all connected. This coupling is manifest in the changes to the CPA medium which occur as the inhomogeneous chemical potential is applied. In the presence of such applied chemical potential change, $\{\delta v_i\}$, the concentration changes $\{\delta c_i\}$ are accompanied by a rearrangement of charge associated with each site, $\{\delta\rho_{i,\,\mathrm{A(B)}}\}$, and by changes to the moments from site to site, $\{\delta\mu_{i,\,\mathrm{A(B)}}\}$. Also, as is well known, there are self-energy effects, which can be very large, associated with the use of Weiss type mean fields. In an effort to improve our mean field theory, as before [7, 8], we have included Onsager cavity field corrections in the calculation of the various correlation functions. These corrections to the mean fields ensure that important sum rules associated with the (diagonal part of the) fluctuation dissipation theorem are satisfied. These alterations, including the Onsager corrections, are all interdependent as shown in the following expressions, where the superscript δc_i refers to the self-energy effect of chemical fluctuations arising from the same site that we are trying to investigate.

$$\delta c_i = \beta c(1-c)\delta v_i^{\mathrm{cavity}}(\{\delta c_j - \delta c_j^{(\delta c_i)}\},\ \{\delta\rho_{j,\,\mathrm{A}} - \delta\rho_{j,\,\mathrm{A}}^{(\delta c_i)}\},$$

$$\{\delta\rho_{j,\mathrm{B}} - \delta\rho_{j,\mathrm{B}}^{(\delta c_i)}\},\ \{\delta\mu_{j,\mathrm{A}} - \delta\mu_{j,\mathrm{A}}^{(\delta c_i)}\},\ \{\delta\mu_{j,\mathrm{B}} - \delta\mu_{j,\mathrm{B}}^{(\delta c_i)}\}) \tag{16}$$

$$\delta\rho_{i,\mathrm{A(B)}}(r_i) = \delta\rho_{i,\mathrm{A(B)}}(r_i;\ \{\delta c_j - \delta c_j^{(\delta c_i)}\},\ \{\delta\rho_{j,\mathrm{A}} - \delta\rho_{j,\mathrm{A}}^{(\delta c_i)}\},$$
$$\{\delta\rho_{j,\mathrm{B}} - \delta\rho_{j,\mathrm{B}}^{(\delta c_i)}\},\ \{\delta\mu_{j,\mathrm{A}} - \delta\mu_{j,\mathrm{A}}^{(\delta c_i)}\},\ \{\delta\mu_{j,\mathrm{B}} - \delta\mu_{j,\mathrm{B}}^{(\delta c_i)}\}) \tag{17}$$

$$\delta\mu_{i,\mathrm{A(B)}}(r_i) = \delta\mu_{i,\mathrm{A(B)}}(r_i;\ \{\delta c_j - \delta c_j^{(\delta c_i)}\},\ \{\delta\rho_{j,\mathrm{A}} - \delta\rho_{j,\mathrm{A}}^{(\delta c_i)}\},$$
$$\{\delta\rho_{j,\mathrm{B}} - \delta\rho_{j,\mathrm{B}}^{(\delta c_i)}\},\ \{\delta\mu_{j,\mathrm{A}} - \delta\mu_{j,\mathrm{A}}^{(\delta c_i)}\},\ \{\delta\mu_{j,\mathrm{B}} - \delta\mu_{j,\mathrm{B}}^{(\delta c_i)}\}). \tag{18}$$

These expressions show that the charge and moment changes must also include the effects of the cavity field corrections. In terms of response functions, (13), (14), and (15), the expressions for the Onsager corrections can be written as

$$\delta c_j^{(\delta c_i)} = \frac{\alpha_{ji}\,\delta c_i}{\beta c(1-c)} \tag{19}$$

$$\delta\rho_{j,\mathrm{A(B)}}^{(\delta c_i)} = \frac{\rho_{ji,\mathrm{A(B)}}\,\delta c_i}{\beta c(1-c)} \tag{20}$$

$$\delta\mu_{j,\mathrm{A(B)}}^{(\delta c_i)} = \frac{\mu_{ji,\mathrm{A(B)}}\,\delta c_i}{\beta c(1-c)} \tag{21}$$

see [7, 14]. That these are reasonable expressions may be evidenced by following fact. If α_{ii} is $\beta c(1-c)$ as required by the fluctuation dissipation theorem to conserve the calculated diffuse intensity, then $\delta c_i^{(\delta c_i)} = \delta c_i$ and there are no self-induced changes due to the site i on the site i, see equations (16), (17), and (18). We shall see that this is indeed so.

From the expressions for the induced changes in the charge and magnetization densities on each site, closed expressions for the various correlation functions can be obtained in terms of quantities based on the electronic structure of the homogeneously disordered alloy [7, 8, 30]. Finally, since the homogeneous state has the symmetry of the lattice, we take the lattice Fourier transforms of equations (13), (14), and (15), namely $\alpha(q)$, $\rho_{\mathrm{A(B)}}^{n}(q)$ and $\mu_{\mathrm{A(B)}}(q)$. We obtain the following key equations:

$$\alpha(q) = \beta c(1-c) + \beta c(1-c)\{(S^{cc}(q) - \Lambda^{c})\alpha(q)$$
$$+ \sum_{n}[S_{\mathrm{A}}^{c\rho;n}(q)\rho_{\mathrm{A}}^{n}(q) + S_{\mathrm{B}}^{c\rho;n}(q)\rho_{\mathrm{B}}^{n}(q)] + S_{\mathrm{A}}^{c\mu}(q)\mu_{\mathrm{A}}(q)$$
$$+ S_{\mathrm{B}}^{c\mu}(q)\mu_{\mathrm{B}}(q) - (S^{cP}(q) + \Delta Q)P(q)C(q)\} \tag{22}$$

$$\rho_{\mathrm{A(B)}}^{n'}(q) = (\epsilon_{\mathrm{A(B)}}^{\rho c;n'}(q) - \Lambda_{\mathrm{A(B)}}^{\rho c;n'})\alpha(q) + \sum_{n}\left[\epsilon_{\mathrm{A,\,A(B)}}^{\rho\rho;n'n}(q)\rho_{\mathrm{A}}^{n}(q) + \epsilon_{\mathrm{B,\,A(B)}}^{\rho\rho;n'n}(q)\rho_{\mathrm{B}}^{n}(q)\right]$$
$$+ \epsilon_{\mathrm{A,\,A(B)}}^{\rho\mu;n'}(q)\mu_{\mathrm{A}}(q) + \epsilon_{\mathrm{B,\,A(B)}}^{\rho\mu;n'}(q)\mu_{\mathrm{B}}(q) - \epsilon_{\mathrm{A(B)}}^{\rho P;n'}(q)P(q)C(q) \tag{23}$$

$$\mu_{\mathrm{A(B)}}(q) = (\chi_{\mathrm{A(B)}}^{\mu c}(q) - \Lambda_{\mathrm{A(B)}}^{\mu c})\alpha(q) + u_1\left[\chi_{\mathrm{A,\,A(B)}}^{\mu\rho;n}(q)\rho_{\mathrm{A}}^{1}(q) + \chi_{\mathrm{B,\,A(B)}}^{\mu\rho;n}(q)\rho_{\mathrm{B}}^{1}(q)\right.$$
$$\left. + \chi_{\mathrm{A,\,A(B)}}^{\mu\mu}(q)\mu_{\mathrm{A}}(q) + \chi_{\mathrm{B,\,A(B)}}^{\mu\mu}(q)\mu_{\mathrm{B}}(q) - \chi_{\mathrm{A(B)}}^{\mu P}(q)P(q)C(q)\right] \tag{24}$$

where $S^{cc}(q)$ etc, $\epsilon_{\mathrm{A(B)}}^{\rho c;n'}(q)$ etc and $\chi_{\mathrm{A(B)}}^{\mu c}(q)$ etc are all determined by the electronic structure of the compositionally disordered, magnetic phase. Explicit expressions using the notation of [7, 8] are given for completeness in appendix A. $P(q) = [c\rho_{\mathrm{A}}^{1}(q) + (1-c)\rho_{\mathrm{B}}^{1}(q)]u_1 + \Delta Q\,\alpha(q)$ is the q dependent variation from charge neutrality, or effective polarization caused by the short-range order, recall u_1 is the normalization constant for the Legendre polynomials. (ΔQ is the net difference in charge when a site is occupied by an A atom and when it is then occupied by a B atom in the homogeneously disordered alloy; we shall

refer to this as the alloy 'charge transfer' even though it is not a precise definition.) $C(q)$ is the lattice Fourier transform of the Coulomb interaction $1/|\boldsymbol{R}_i - \boldsymbol{R}_j|$.

Similarly, the lattice Fourier transforms of the Onsager cavity corrections Λ^c, $\Lambda^{\rho c;n'}_{A(B)}$ and $\Lambda^{\mu c}_{A(B)}$ can be written as follows,

$$\Lambda^c = \frac{1}{\beta c(1-c)} \int \mathrm{d}q \left[S^{cc}(q)\alpha(q) + \sum_n (S^{c\rho;n}_A(q)\rho^n_A(q) + S^{c\rho;n}_B(q)\rho^n_B(q)) + S^{c\mu}_A(q)\mu_A(q) + S^{c\mu}_B(q)\mu_B(q) - (S^{cP}(q) + \Delta Q)P(q)C(q) \right] \tag{25}$$

$$\Lambda^{\rho c;n'}_{A(B)} = \frac{1}{\beta c(1-c)} \int \mathrm{d}q \left[\epsilon^{\rho c;n'}_{A(B)}(q)\alpha(q) + \sum_n (\epsilon^{\rho\rho;n'n}_{A,A(B)}(q)\rho^n_A(q) + \epsilon^{\rho\rho;n'n}_{B,A(B)}(q)\rho^n_B(q)) + u_1\epsilon^{\rho\mu}_{A,A(B)}(q)\mu_A(q) + u_1\epsilon^{\rho\mu}_{B,A(B)}(q)\mu_B(q) - \epsilon^{\rho P;n'}_{A(B)}(q)P(q)C(q) \right] \tag{26}$$

$$\Lambda^{\mu c}_{A(B)} = \frac{1}{\beta c(1-c)} \int \mathrm{d}q \left[\chi^{\mu c}_{A(B)}(q)\alpha(q) + \sum_n (\chi^{\mu\rho;n}_{A,A(B)}(q)\rho^n_A(q) + \chi^{\mu\rho;n}_{B,A(B)}(q)\rho^n_B(q)) + u_1\chi^{\mu\mu}_{A,A(B)}(q)\mu_A(q) + u_1\chi^{\mu\mu}_{B,A(B)}(q)\mu_B(q) - \chi^{\mu P}_{A(B)}(q)P(q)C(q) \right] \tag{27}$$

in which we have used similar prescriptions to set up these corrections as in [7, 19] in which the notion of Onsager cavity fields is incorporated in a consistent manner to the way in which we treat the electronic structure. It is important to note that the sum rules $\int \alpha(q)\,\mathrm{d}q = \alpha_{ii} = \beta c(1-c)$, $\int \rho^{n'}_{A(B)}(q)\,\mathrm{d}q = 0$ and $\int \mu_{A(B)}(q)\,\mathrm{d}q = 0$ are satisfied naturally by this construct and not imposed from the outset. The compositional correlation function $\alpha(q)$, or Warren–Cowley short-range order parameter, is obtained from the solution to the six equations shown above and has the Ornstein–Zernicke form

$$\alpha(q) = \frac{\beta c(1-c)}{1 - \beta c(1-c)[S^{(2)}(q;\{\Lambda\}) - \Lambda^c]}. \tag{28}$$

$S^{(2)}(q)$ is determined by the solution of the coupled equations for $\alpha(q)$, $\rho^{n'}_{A(B)}(q)$, $\mu_{A(B)}(q)$, Λ^c, $\Lambda^{\rho c;n'}_{A(B)}$ and $\Lambda^{\mu c}_{A(B)}$ shown above and all equations are dependent on quantities determined by the electronic structure of the homogeneously disordered alloy (see appendix A). We note also that the conservation of the calculated diffuse intensity is *not* established by the naive integration of $\alpha(q)$ over all reciprocal space to force $c(1-c)$. The effective chemical interaction $S^{(2)}(q) - \Lambda^c$ is dependent not only on the constant Λ^c but also q dependent Onsager corrections arising from the charge and magnetization terms normally neglected in other mean field theories. This subtlety has been missed in the past.

For interpretation purposes the 'interchange' energy $S^{(2)}(q)$ can ultimately be broken up into three components, i.e.

$$S^{(2)}(q) = S^{cc}(q) + S^{\mathrm{cross}}(q) - \frac{(\Delta Q)^2 C(q)}{[1 + l^2_{\mathrm{scr}}C(q)]}. \tag{29}$$

The first term derives from the filling of the electronic states and has been discussed at length by several authors when spin fluctuation effects and other magnetic effects are neglected [26, 31, 32]. It relates to the Hume-Rothery electron per atom ratio rule. The other two terms describe the contributions to the interchange energy which occur as the charge and local moment magnitudes rearrange as a consequence of the atomic short-range order. The second of these two terms describes an electrostatic ('charge transfer'-like) piece and depends on the Coulomb interaction $C(q)$ and an inverse screening length l^{scr} which is also

determined by the electronic structure. Such effects for alloys in which magnetic effects are unimportant have been discussed in the two earlier articles [7, 8] and for paramagnetic alloys in which spin fluctuation effects are handled to some extent by Ling *et al* [9]. For a ferromagnetic alloy, these quantities are dependent on the nature of the spin polarization of the electronic structure of the compositionally disordered alloy.

3. Magnetocompositional effects

In this section, we turn our attention to studying the response of the local magnetization to the of application of a concentration wave. Starting from equation (8) and considering the effects upon the CPA effective medium, we can define an expression for the change of magnetization at site i, $\delta\mu_i(r_i)$, caused by a change of concentration at site j, γ_{ij}, i.e.

$$\gamma_{ij} = \frac{\delta\langle\mu_i\rangle}{\delta c_j} = \frac{\delta(c_i\mu_i^{\mathrm{A}} + (1-c_i)\mu_i^{\mathrm{B}})}{\delta c_j} = (\bar{\mu}^{\mathrm{A}} - \bar{\mu}^{\mathrm{B}})\delta_{ij} + c\frac{\delta\mu_i^{\mathrm{A}}}{\delta c_j} + (1-c)\frac{\delta\mu_i^{\mathrm{B}}}{\delta c_j} \tag{30}$$

in which the bars refer to the homogeneous CPA averages. We shall designate the latter two quantities γ_{A}^{ij} and γ_{B}^{ij}. The lattice Fourier transform of this equation is $(\mu_{\mathrm{A}} - \mu_{\mathrm{B}}) + c\gamma_{\mathrm{A}}(q) + (1-c)\gamma_{\mathrm{B}}(q)$. The quantities $\gamma_{\mathrm{A}}(q)$ and $\gamma_{\mathrm{B}}(q)$ are available in terms of electronic structure dependent quantities of the form

$$\gamma_{\mathrm{A(B)}}(q) = \gamma^m_{\mathrm{A(B)}}(q) + \frac{\kappa^m_{\mathrm{A(B)}}(q)[cu_1\gamma^1_{\mathrm{Ac}}(q) + (1-c)u_1\gamma^1_{\mathrm{Bc}}(q) + \Delta Q]}{C^{-1}(q) - u_1[c\kappa^1_{\mathrm{Ac}}(q) + (1-c)\kappa^1_{\mathrm{Bc}}(q)]} \tag{31}$$

where $\gamma^n_{\mathrm{A(B)c}}(q)$, $\gamma^m_{\mathrm{A(B)}}(q)$, $\kappa^n_{\mathrm{A(B)c}}(q)$ and $\kappa^m_{\mathrm{A(B)}}(q)$ given in appendix B. It is important to note that the magnetization changes are accompanied by rearrangement of charge and this has been fully accounted for in the derivation of the above expressions.

The above quantity is important because it determines the 'local' chemical environment effects to the moments. Moreover, the magnetocompositional correlation function $\Upsilon(q)$, i.e.

$$\Upsilon(q) = (1/N)\sum_j \beta(\langle\mu_i\xi_j\rangle - \langle\mu_i\rangle\langle\xi_j\rangle)\exp(\mathrm{i}q\cdot(R_i - R_j)) \tag{32}$$

can be expressed in terms of these response functions as

$$\begin{aligned}\Upsilon(q) &= \frac{1}{N}\sum_j \left(\frac{\delta\langle\mu_i\rangle}{\delta v_j}\right)\exp\left(\mathrm{i}q\cdot(R_i - R_j)\right) \\ &= \frac{1}{N}\sum_{jk}\left(\frac{\delta\langle\mu_i\rangle}{\delta c_k}\right)\left(\frac{\delta c_k}{\delta v_j}\right)\exp\left(\mathrm{i}q\cdot(R_i - R_j)\right) = \gamma(q)\alpha(q).\end{aligned} \tag{33}$$

It is the quantities $\Upsilon(q)$ and $\alpha(q)$ that are determined in diffuse neutron scattering, thereby indirectly finding $\gamma(q)$, as discussed in the introduction.

3.1. Moment–compositional response

If we focus upon $\gamma(q)$, we note that it describes quintessentially a non-rigid, itinerant moment effect due to changes in the compositional environment; hence, we will refer to $\gamma(q)$ as the moment–compositional (MC) response. The $\gamma_{ij}^{\mathrm{A(B)}}$ (equation (30)) have a particularly revealing physical interpretation. They describe the change in the size of the moment on a site i in the lattice if it is occupied by an A (B) atom and if the probability of occupation is altered on another site j. Thus,

$$\gamma_{ij}^{\mathrm{A(B)}}\Delta c_j = \gamma_{ij}^{\mathrm{A(B)}}(1-c) \tag{34}$$

describes the change in the moment on the site i, occupied by an A (B) atom, if the site j in the alloy is now definitely occupied by an A atom. Similarly,

$$\gamma_{ij}^{A(B)}\Delta c_j = \gamma_{ij}^{A(B)}(-c) \tag{35}$$

describes the changed if the site j is now definitely occupied by a B atom. In practice, equations (34) and (35) are used with the site i fixed and the label j running over each shell of nearest neighbours. Henceforth, only the shell label is necessary for the γ. Thus, if a_j (b_j) represents the number of A (B) atoms in the jth shell, then $\mu^{A(B)}$ due to the new local environment (a_1, b_1; a_2, b_2; ...) is given by

$$\mu_\alpha = \bar{\mu}_\alpha^{CPA} + \sum_j \gamma_j^\alpha \left[(1-c)a_j + (-c)b_j\right] \tag{36}$$

where α represents A (B) and runs over all pertinent shells.

Consequently, once the MC response functions have been calculated, it is possible from equation (36) to investigate, in a perturbative fashion, the magnetic structure of alloys of varying chemical environment. Hence, it provides a complementary approach to that supplied by explicit cluster calculations [33]. In fact, albeit a perturbative method, it is a susceptibility based calculation and, as long as the induced moments are relatively small, a qualitative, if not quantitative, description may be possible. Thus, the magnetic properties of modulated or clustering alloys can be examined and alloys can be designed theoretically to have specified magnetic properties, without any further computational effort.

The lattice Fourier transform of the $\gamma^{A(B)}(q)$, $\gamma_{ij}^{A(B)}$, may be estimated via equation (30) using a distribution of q vectors and, sometimes, is found to be fairly short ranged. That is, the functional form of $\gamma(q)$ is cosine-like between $q = 0$ and the zone boundary and the major contribution to γ_i comes from the first-nearest-neighbour shell. For alloys with this behaviour, the putative locality of the changes in the magnitude of the moments is given theoretical justification. On the other hand, any deviation from the cosine form implies that more shells of atoms will be involved in change in the moment.

4. Applications

To illustrate the information contained in the MC response functions, we present the results of calculations on two bulk Fe–V and Cr–Fe alloys. These calculations were performed at lattice constants near the experimental ones, although we could have performed total energy calculations for the disordered alloy to determine the theoretical minimum as done by Johnson *et al* [22]. Recall that in some systems, such as the Invars, where magnetovolume coupling has a large effect, determination of the volume could be very important to $\gamma(q)$. Following the discussion of the MC response function in these two alloys, we utilize the linear response equation, equation (36), to investigate layered structures. Further aspects of our calculations for these systems and several other alloys will be published elsewhere.

4.1. The bulk alloys

Figures 1 and 2 show the spin polarized electronic density of states of the compositionally disordered, magnetic $Cr_{70}Fe_{30}$ and $Fe_{87}V_{13}$ alloys. In the $Fe_{87}V_{13}$ alloy, average moments of $2.075\mu_B$ and $-0.724\mu_B$ are set up on the Fe and V sites, respectively. Average moments of $0.014\mu_B$ and $2.047\mu_B$ are found for the Cr and Fe sites in $Cr_{70}Fe_{30}$. Note that neither the majority nor the minority spin states are fully occupied and they are not rigidly exchange split. Notions of 'covalent magnetism' [34] are relevant here. Both show the majority spin

states to be strongly affected by the compositional disorder in contrast to the minority spin states. (The opposite is the case for $Ni_{75}Fe_{25}$ for example [2].)

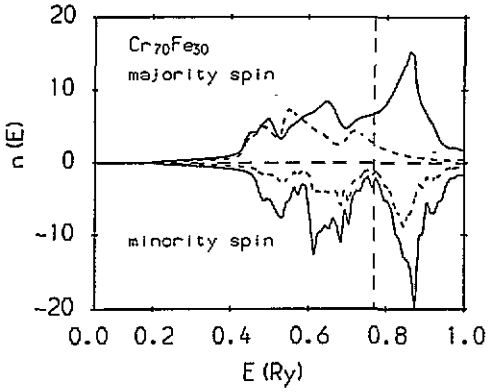

Figure 1. The compositionally averaged densities of the majority and minority states of $Cr_{70}Fe_{30}$ and its resolution into Cr (solid) and Fe (dashed) components weighted by concentration, in units of states Ryd^{-1}/(atom spin).

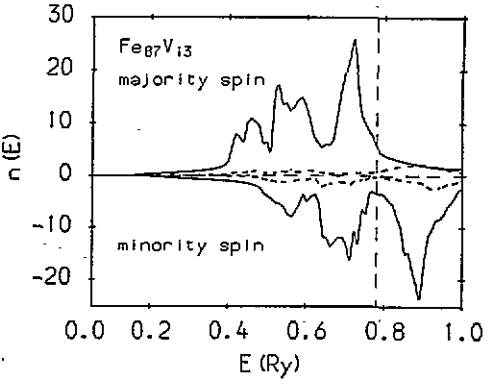

Figure 2. Same as in figure 1, except for $Fe_{87}V_{13}$ and its resolution into Fe (solid) and V (dashed) components.

We show the Cr and Fe components of $\gamma(q)$ in the $q_z = 0$ plane for $Cr_{70}Fe_{30}$, with $\gamma_{Cr}(q)$ in figure 3(a) and $\gamma_{Fe}(q)$ in figure 3(b). An incommensurate peak is evident in $\gamma_{Cr}(q)$ which demonstrates the long-ranged nature of the dependence of the magnetization on Cr sites on their compositional environment. The incommensurate peak in $\gamma(q)$ means that it can only be fitted by many real space parameters, $\gamma_{ij}^{A(B)}$. This is contrary to the case of $Fe_{87}V_{13}$ in which the dominant contribution come from the first two shells only, $\gamma_1^{Fe} = 0.096\mu_B$, $\gamma_2^{Fe} = 0.047\mu_B$, $\gamma_1^{V} = -0.165\mu_B$ and $\gamma_2^{V} = -0.057\mu_B$. This short-ranged nature means that the magnetization of a variety of compositionally modulated Fe–V alloys (compositionally modulated systems—CMS) can be simulated using these quantities and equations (34), (35) and (36).

Cable and coworkers carried out some unpolarized neutron scattering measurements on a single crystal of $Fe_{87}V_{13}$ [35]. We found excellent agreement between our calculations of $\alpha(q)$ and these data [30]. We were also able to provide an analysis in terms of the underlying electronic structure of the alloy. Cable *et al* [36] have since carried out polarized neutron

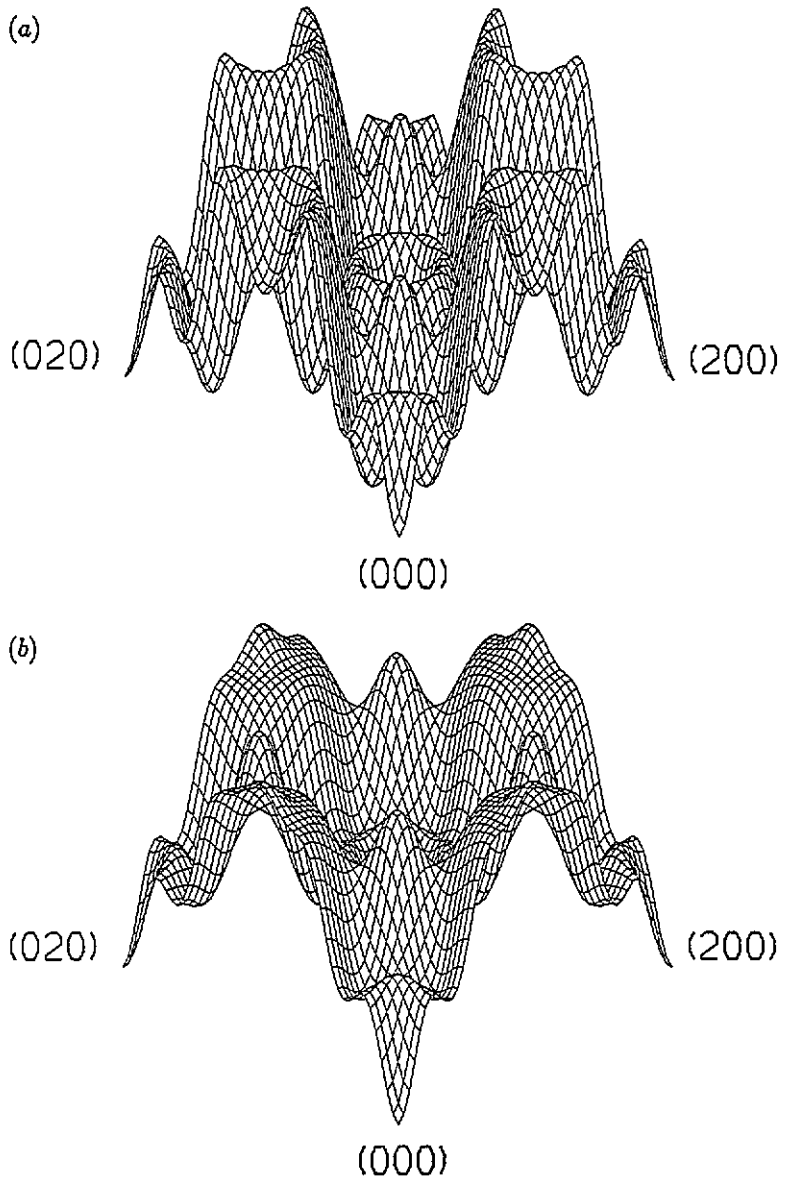

Figure 3. Surface plot of the (a) Cr and (b) Fe component of the magnetocompositional function, $\gamma(\mathbf{q})$, of $Cr_{70}Fe_{30}$ at 600 K for the $q_z = 0$ plane in atomic units.

scattering measurements on the crystal along the three high-symmetry directions, i.e. [100], [110] and [111]. We compare the calculated $\gamma(q) = [\mu_A - \mu_B] + c\gamma_{Fe}(q) + (1-c)\gamma_V(q)$ along the same symmetry directions with these data in figures 4(a), 4(b) and 4(c). In addition, the bulk measurement of the magnetic moment by Aldred [37] is also shown on the same plots at $|q| = 0$. Note that our calculation is in good, qualitative agreement with experimental data of Cable *et al*. In figures 4(a) and 4(b), we can see the cosine-like variation in both our calculation and experimental data. More strikingly, in figure 4(c), we have also reproduced the experimentally observed double peak along the [111] direction.

We attribute the second peak to the effect of Fermi surface nesting with a '$2k_F(111)$' nesting vector in the majority spin Fermi surface, which also characterizes the double peak in $\alpha(q)$ as detailed in [30]. It is important to note that the measurement of Aldred is not dependent on all the subtle effects that have to be accounted for when performing the spin polarized neutron scattering, e.g., effects of crystal surface (inhomogeneities), alignments of crystal axes to the spectrometer and, most importantly, the degree of polarization of the neutron beam. In this regard, we have very good quantitative agreement with the more confident $q = 0$ value and good agreement with the q dependence found in the neutron experiment, excepting that the difference in maximum and minimum values of the function seem larger in the experiment.

Mirebeau *et al* [15] carried out polarized neutron measurements on polycrystalline Fe_cV_{1-c} alloys for a range of concentrations. They fitted their measured average moment disturbance ϕ_i on the ith nearest-neighbour shell to an expression of the form:

$$M(K) = \Delta\mu + \sum_i N_i \phi_i \frac{\sin(K \cdot R_i)}{(K \cdot R_i)} \tag{37}$$

where $\Delta\mu = \bar{\mu}_A - \bar{\mu}_B$ is the difference of the average magnetic moments carried by iron and vanadium moments, respectively; N is the number of nearest neighbours in the ith shell. $M(K)$, $\Delta\mu$ and ϕ_i are expressed in μ_B/atom and the scattering vector K in Å^{-1}. We use equation (37) to calculate $M(K)$ using the average of our real space shell fits, i.e. $\phi_i = c\gamma_i^{Fe} + (1-c)\gamma_i^{V}$ $(i = 1, 10)$, and the results are presented in figure 5. Once again, our $M(K)$ agrees well with Aldred's measurement at $K = 0$ and exhibits the same general oscillatory behaviour as the plot for $Fe_{0.853}V_{0.147}$ in figure 1 of [15].

A good description of the moments of Fe_cV_{1-c} alloys has been given by several authors [38, 5, 39, 40] with very good agreement to neutron scattering results. In particular, FeV alloys are ferrimagnetic, i.e. the vanadium polarization is antiparallel to the iron polarization. The magnetism in these alloys is different from, say, NiFe alloys because the moments on vanadium atoms are induced due to the large exchange splitting of the iron atoms. This leads to large local environment effects, which, again, may be investigated through the present formalism.

Moments on both the iron and vanadium sites increase (decrease) in magnitude if their environment contains more iron (vanadium) atoms. Intuitively, one should expect this behaviour since the vanadium moment is an induced moment. The collapse of the moments at 70% vanadium in the FeV system is an immediate consequence of a vanadium rich environment [38, 5, 39, 40]. Although a calculation using equation (36) results in a large reduction in the size of the iron and vanadium moments (for iron, $2.08\mu_B$ to $1.16\mu_B$ for a (0, 8; 0, 6) environment), it does not describe properly, being a perturbative method, the magnetic collapse that occurs in the $V_{0.70}Fe_{0.30}$ random alloy. That is, it is improbable that perturbative extrapolation from a V–87% Fe alloy will give good results for a critical behaviour occurring in V–30% Fe alloy. However, no critical collapse of the moments is seen experimentally in the Fe/V CMS. As a result, Fe/V CMSs are the focus of our study using the MC response functions for this system.

4.2. Compositionally modulated structures

Obviously, physical properties of modulated structures will be influenced by the details of the various atomic configurations at the interfaces. It is also highly probable that alloying of some sort will occur at the CMS interfaces which will distinguish those atoms in and near the interface layers. As such, we use the MC response functions to illustrate their

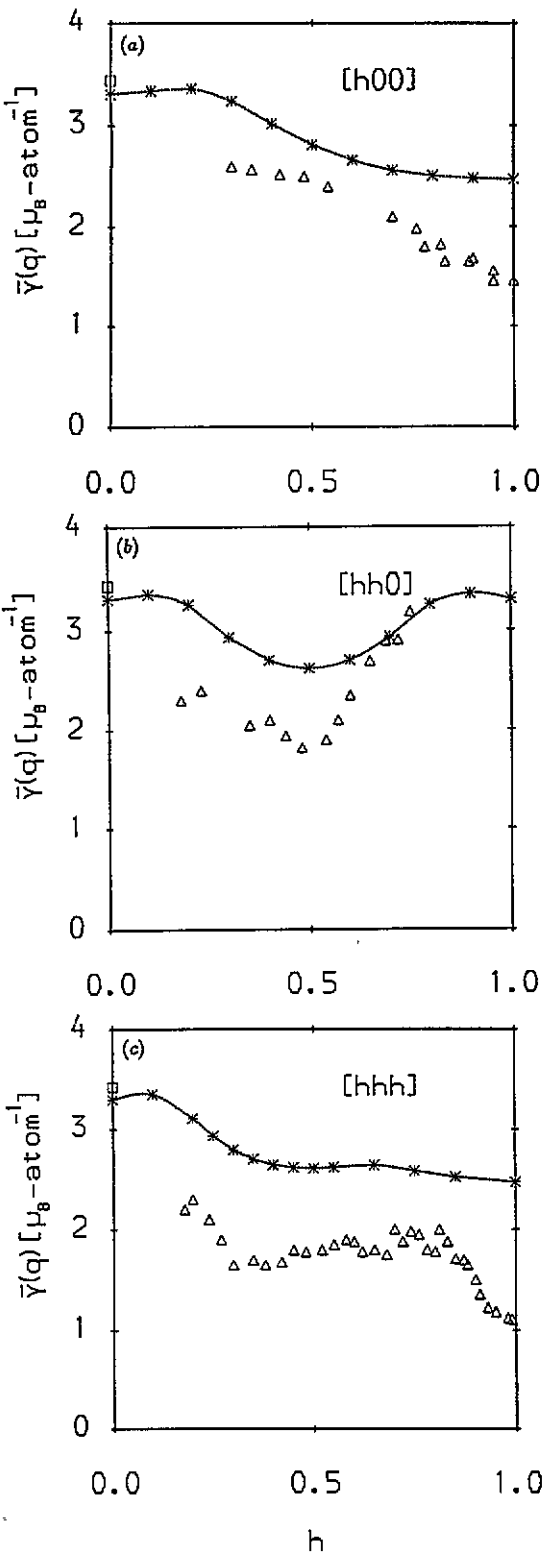

Figure 4. Variation of magnetocompositional function, $\gamma(q)$, for ferrimagnetic $Fe_{87}V_{13}$ along the symmetry direction (a) [100], (b) [110] and (c) [111], in units of μ_B per atom. Stars: our results; triangles: data from Cable *et al* [36]; square: Aldred's measurement [37].

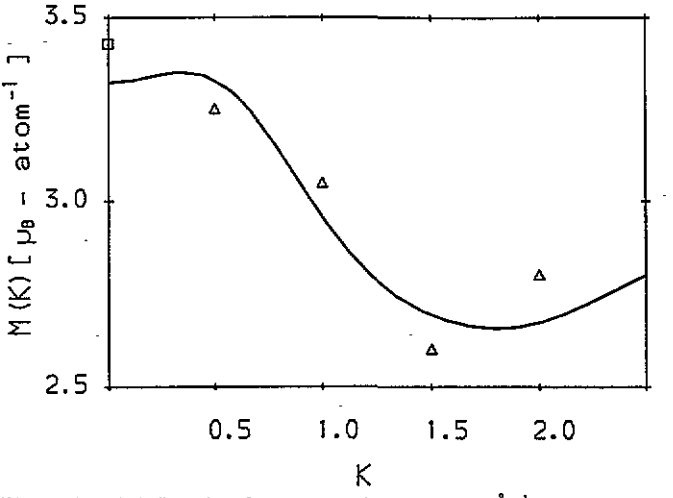

Figure 5. $M(K)$ (in units of μ_B per atom) versus K (in Å^{-1}). Solid line: our calculation using equation (37); square: Aldred's result [37]; triangles: points at $K = 0.5$, 1.0, 1.5 and 2.0 from the plot for $Fe_{0.853}V_{0.147}$ in figure 1 of [15].

utility for obtaining information on CMSs. With the γ_i calculated, one must only provide a configurational environment in order to use equation (36).

Recall these calculations are based on the disordered alloy where a global exchange splitting has been established. $\gamma(q)$ provides information on the local enhancement to the exchange splitting due to the change in the chemical environment. Whether this should apply when one is investigating a CMS which has a dramatic change in the 'concentration' should be based on the strength of the perturbation.

The FeV alloys are systems well known to exhibit environmental effects and have been studied extensively, both experimentally and theoretically, especially in superlattice structures. This is probably due to the fact that Fe and V have similar BCC lattice constants leading to the possibility of epitaxial growth with a simple lattice structure and of having ideal modulation between the Fe and V layers. In fact, x-ray diffraction analysis has shown that the Fe/V CMS have a [110] texture and Mössbauer experiments indicate that the concentration profile at the interface between Fe and V is sharp with alloying confined to three interface layers [41].

Several important chemical environment effects in Fe/V CMSs have been measured which may be compared with the present results. Using polarized neutron scattering, Hosoito *et al* [4] deduced a 30% reduction of the interface Fe moment in the thick Fe/V CMS. Assuming a weak vanadium moment, Jaggi *et al* [3] found no magnetically dead layers of Fe. In fact, as the number of Fe layers was decreased the average iron moment also decreased. Moreover, it was concluded from ^{51}V hyperfine field measurements that the interface layer was an alloy of $Fe_{0.50}V_{0.50}$.

Other theoretical investigations on Fe/V CMSs have been done; namely self-consistent, LAPW electronic structure calculations have been performed by Hamada *et al* [5] on an ideal FeV superlattice with the [100] and the [110] textures. They found reduced moments for the interface iron layer and small negative moments on the interface vanadium. An interpretation based on local composition about the interface region was put forth from the FeV alloy model calculation of Hamada and Miwa [5].

Also, Elzain *et al* [42] have performed calculations on Fe/V superlattices based on 15-atom clusters for the magnetic moment and hyperfine field trends. Due to the size of the cluster, moments and hyperfine field values are discrepant with larger cluster calculations. More importantly, they found that the iron moments grow with a vanadium rich environment. This is in contradiction to our calculation and experiments on thick Fe/V superlattices. However, this disagreement may possibly be explained by noting that their calculations were on superlattices with 'ultrathin' iron layers, and that Wong *et al* [43] have observed two-dimensional behaviour in some ultrathin iron layers. In such a situation, it is possible that the present theory, based on bulk correlations, would break down. Also, calculations in which vanadium was taken as a central atom were not performed by Elzain *et al*, so their conclusions on vanadium were more uncertain and we make no comparison. Qualitatively, by considering the configurational environment (a_1, b_1; a_2, b_2) for the BCC structure, we concluded previously for $Fe_{0.87}V_{0.13}$ that the magnitudes of both the iron and vanadium local moment increase (decrease) for increasing a_1 (b_1) and a_2 (b_2). Recall, this is due to the negative polarization of the vanadium moments.

A further bit of information may be obtained indirectly from the induced moments. Since the moments are related to the occupation of the majority and minority density of states, the reduction (growth) in the iron (vanadium) moments in the interface layers requires the transferring of electrons from the iron majority spin manifold to the vanadium minority spin manifold. This behaviour was observed in the calculation of Hamada *et al*. It will be more striking for the stacking with the less closely packed planes, such as the [100] stacking.

4.2.1. [110] textures. In tables 1 and 2 the possible environmental configurations for any [110] modulation which involve contributions from only two nearest-neighbour shells are given, along with the induced and local moments on the iron and vanadium sites. For the [110] texture, Hamada *et al* [5] calculated two different stacking sequences, 3V/3Fe (V–V–Fe–Fe–Fe–V) and 5V/Fe (V–V–V–Fe–V–V), where in parentheses we denote the unit cell. For case 1, there are two inequivalent iron and vanadium sites, whereas for case 2, there are three inequivalent vanadium sites and one iron site. Their values are compared in table 3 with the values obtained from equation (36). Note that the qualitative trends agree well but, due to the higher iron concentration in our calculation, the local moments in the iron rich planes, i.e. Fe(I), Fe(II) and Fe(III), give much better agreement than those in the V rich planes. Also, the agreement is better for case 1 than case 2. This is perhaps due to a breakdown of the present theory for ultrathin layers, i.e. the iron and vanadium atoms in the single layer may be exhibiting two-dimensional behaviour which would not be properly described. Overall, for thicker multilayers anyhow, if only magnetic moments are of interest, no further calculations are required to generate some other stacking sequence, in contrast to other electronic structure calculations.

Table 1. Including effects from two nearest-neighbour shells only, the stacking sequence, environmental configuration, change of moment and total moments for sites in a central Fe plane are presented for an FeV multilayer with a [110] texture.

Local stacking	Environment	$\Delta\mu$	μ^{Fe}
–Fe–Fe–Fe–	(8, 0; 6, 0)	0.13	2.21
–Fe–Fe–V–	(6, 2; 4, 2)	−0.15	1.92
–V–Fe–V–	(4, 4; 2, 4)	−0.44	1.63

Table 2. Including effects from two nearest-neighbour shells only, the stacking sequence, environmental configuration, change of moment and total moments for sites in a central V plane are presented for an FeV multilayer with a [110] texture.

Local stacking	Environment	$\Delta\mu$	μ^{V}
–Fe–V–Fe–	(4, 4; 4, 2)	0.57	-0.16

4.2.2. [100] textures. Hamada *et al* [5] investigated a [100] texture with a stacking sequence given by three layers of V and five layers of Fe. Note, for this sequence, there are two (three) inequivalent vanadium (iron) atoms. Tables 4 and 5 provide similar information for the [100] texture to that of tables 1 and 2 for the [110] texture, with the first three configurations relevant to the stacking sequence of Hamada *et al* which are shown as case 3 in table 3. Note that the trend is again given well by this method of MC response with excellent agreement in the Fe rich planes; however, the moment oscillation that they calculated is not obtained. It would be possible to achieve a moment oscillation only if the second shell γ_2 was of opposite sign. Or, equally true, it may be due to a slight error in the calculation of Hamada *et al*. Experimentally, Jaggi *et al* rule out the possibility of an oscillatory behaviour of the iron moments, in agreement with our results.

Table 3. A comparison is made between moments calculated via the response functions (left-hand column) and actual supercell electronic structure calculations (right-hand column) of Hamada *et al* [5].

Site/plane	Case	1	Case	2	Case	3
Fe (I)	1.92	1.90	1.63	1.33	1.78	1.62
Fe (II)	2.21	2.20			2.16	2.39
Fe (III)					2.21	2.21

Table 4. Including effects from two nearest-neighbour shells only, the stacking sequence, environmental configuration, change of moment and total moments for sites in a central Fe plane are presented for an FeV multilayer with a [100] texture.

Local stacking	Environment	$\Delta\mu$	μ^{Fe}
–Fe–Fe–Fe–Fe–Fe–	(8, 0; 6, 0)	0.13	2.21
–Fe–Fe–Fe–Fe–V–	(8, 0; 5, 1)	0.08	2.16
–V–V–Fe–Fe–Fe–	(4, 4; 5, 1)	−0.30	1.78
–V–Fe–Fe–Fe–V–	(8, 0; 4, 2)	0.04	2.12
–Fe–Fe–Fe–V–Fe–	(4, 4; 6, 0)	−0.25	1.83
–Fe–V–Fe–V–Fe–	(0, 8; 6, 0)	−0.64	1.44
–Fe–V–Fe–V–V–	(0, 8; 5, 1)	−0.68	1.40

We note that a [112] texture is also a possible modulation and, using γ values from two nearest-neighbour shells, there are nine possible environments; however, here we simply note that it is possible to investigate the consequences of this texture as well using our approach.

Table 5. Including effects from two nearest-neighbour shells only, the stacking sequence, environmental configuration, change of moment and total moments for sites in a central V plane are presented for an FeV multilayer with a [100] texture.

Local stacking	Environment	$\Delta\mu$	μ^V
–V–Fe–V–Fe–V–	(8, 0; 0, 6)	0.14	−0.58
–V–Fe–V–Fe–Fe–	(8, 0; 1, 5)	0.08	−0.64
–Fe–Fe–V–V–Fe–	(4, 4; 2, 4)	0.68	−0.04
–Fe–Fe–V–Fe–Fe–	(8, 0; 2, 4)	0.02	−0.70

4.2.3. Concepts of 'local' concentration. Hamada *et al* [5] interpreted their LAPW results in terms of the local environment effects of Hamada and Miwa [5]. They proposed that alloy theory could be used to predict moments in superlattice structures if the magnetic moment of a given atom is determined within a certain 'magnetic interaction' distance, arbitrarily chosen to be the second-nearest-neighbour distance, and if the concentration of the alloy is regarded as the 'local' concentration defined by the percentage of next-nearest-neighbour vanadium. The number of vanadium atoms in the first-nearest-neighbour shell was used to determine the immediate environment.

From the present results, it is now clear why their prescription worked well for FeV heterostructures. Firstly, the γ_1 and γ_2 give the dominant contribution to the environmental effects, which justifies the Hamada *et al* assumption of a magnetic 'interaction length' confined only to the first-two-neighbour shells. Secondly, their calculation explicitly accounts for the effect on the moments due to various first shell occupancies. In the present case, this is done implicitly by γ_1. Thirdly, the 'local' concentration they define gives information that is similar to the γ_2 contribution to equation (36), that is, the second-shell environment and enhancement. So the nearest-neighbour environment and the 'local' concentration are really related to the perturbation Δc_1 and Δc_2, respectively, about a given disordered state. Thus, the Hamada *et al* prescription should not necessarily work for other systems, such as CrFe where the number of contributing shells is large. The MC response determines its applicability.

4.2.4. Interfacial alloying. Experimentally, it is most probable that the interfacial layers will not be ideal; hence some alloying should be expected within a few interface planes. This was the case experimentally for the FeV system, as previously mentioned. Applying standard band structure approaches to the interfacial alloying problem remains a rather difficult and computationally taxing problem. However, using the present theory, it is possible to estimate roughly the effects of alloying on the interfacial layers without any added computational effort.

For example, in the [110] texture of FeV, the three planes composing the ideal interface can be denoted by Fe–Fe–V, with the environment for the iron atom in the central and next layer given by (6, 2; 4, 2) and (8, 0; 6, 0), respectively. The induced interface and first-layer iron moments are $1.92\mu_B$ and $2.21\mu_B$ respectively. Assuming a random 50/50 alloying for the interface plane as given by experiment, i.e. Fe–(FeV)–V, the environment for the iron atom in the interface and next plane changes to (4, 4; 3, 3) and (7, 1; 5, 1), respectively, which results in reduced Fe moments due to a more V rich environment. Consequently, the iron moments are now $1.68\mu_B$ and $2.06\mu_B$, respectively. Compared to the pure Fe moment the ideal (alloyed) interface sees a 7.5% (19%) decrease in the Fe moment. For contrast, an ordered 50/50 interface gives an Fe environment of (2, 6; 2, 4) and an Fe moment

of $1.44\mu_B$, i.e. a moment reduction of 31%. Jaggi *et al* measured an approximately 30% decrease. Therefore, in comparison to experiment, our calculation supports a near-ordered interface. This sort of comparison between experiment and theory should be beneficial in interpreting the actual properties of multilayers.

4.3. Source of error

The calculation of magnetic properties of alloys due to change in the chemical environment may be criticized in several ways. Firstly, the γ_i have been only determined approximately from a selection of q vectors (40 for $Fe_{87}V_{13}$ and 45 for $Cr_{70}Fe_{30}$ in this work), and in some interfaces, including more values may change the inference about the number of shells contributing. Secondly, since the γ_i were calculated from the disordered state ($c = 0.87$), the large deviations of Δc_1 from the disordered configurations needed to obtain the modulated structures might cause the perturbative approach to break down. Thirdly, the explicit volume dependence has been neglected. The CMS could have magnetic moments affected through differences in lattice parameters, which, in turn, should affect the γ_i , as is found in some NiFe thin films. Along the same line, displacement effects that remove the rigid-lattice constraint could also play an important role in systems that have differing atomic 'sizes'. Thus, mostly qualitative information should be expected.

4.4. Hyperfine field—chemical response

Experimentalists have commonly assumed that the hyperfine fields (HFFs) for the species α, B_α, are related to the local magnetic moment μ_α and the average magnetic moment $\bar{\mu}$. For example, Johnson *et al* [44] suggested that the HFF of Fe for several iron based, transition metal alloys could be reproduced by $B_{Fe} = a\mu_{Fe} + b\bar{\mu}$. These authors found, however, that no set of parameters a and b could satisfy this relation. On the other hand, Erich [45] found that he could use this relation for NiFe alloys if he assume that the first (second) term was due to core (conduction) electrons. Theoretically, using a cluster KKR–CPA, Ebert *et al* [46] calculated HFFs with overall agreement with experiment and finds no such relation to hold.

Moreover, for Fe_cNi_{1-c} alloys, Ebert *et al* found changes of the HFF ΔB_α^i with respect to configuration of each shell to be nicely additive. (Note, ΔB_α^i are equivalent to $(\delta B/\delta c)^i$, in analogy to γ_i.) Consequently, they deduced that the hyperfine field at the central site may be expressed by

$$B_\alpha = B_\alpha^{CPA} + \sum_i \Delta B_\alpha^i (n_{Fe}^i - \bar{n}_{Fe}^i) \tag{38}$$

where n_{Fe}^i and $\bar{n}_{Fe}^i$ are the actual and average number of iron atoms in this shell i, respectively, and B^{CPA} is the CPA result. A primary result was that ΔB_α^i does <u>not</u> vanish for shells beyond the second-nearest neighbour; in fact, there is an oscillatory behaviour. Similar results were obtained for other iron based alloys.

Two points are of major importance. Firstly, although it is not presented here, it is possible to derive within the KKR–CPA formalism the effect of changes of the concentration on *any* 'local' quantity related to the Green function, such as the hyperfine fields, Knight shifts, isomer shifts, or the moments, as we have done. Without going through the derivation, one may infer the supposed relation for the hyperfine fields from the explicit calculations of Ebert *et al*. This is fairly obvious from equation (38) since the number of Fe atoms is proportional to concentration. Using the notation in their equations, we may rewrite

equation (38) as

$$B_\alpha = B_\alpha^{\mathrm{CPA}} + \sum_i \Delta B_\alpha^i \left((1-c)a_i + (-c)b_i\right) \tag{39}$$

since $c(a_i + b_i)$ is the average number of iron atoms in the ith shell. This equation is entirely equivalent to that obtained for the moment–chemical response, equation (36). Of course, all the results of Ebert *et al* follow.

Secondly, it is clear from their results that the ΔB, i.e. $(\delta B/\delta c)$, are fairly linear in concentration. Notably, if we assume that the local moments scale with the concentration fluctuations in the same way as the local hyperfine fields, the results of Ebert *et al* can be interpreted as implying that equation (36) is useful when δc_i is not small. Of course, in regions of criticality this may no longer be true, and explicit calculations in that region will be necessary. As can be done for the moments via equation (36), equation (39) may then be used to investigate the effect of various environmental configurations, such as those due to ASRO or to multilayer configurations, on the HFF.

Other work on the environmental effects on the HFF has been done by Hamada *et al* [47]. By assuming ASRO to be only relevant in the first shell and the HFF determined by moments up to the second shell, they used an empirical approach based on their alloy moment calculations to investigate hyperfine field changes in FeV alloys and superlattices and to extract ASRO information from Mössbauer measurements. Overall good agreement was obtained between theory and experiment. Similar comparisons to that given in the previous section on moment responses may be made between our two approaches on HFF. Our results rely on *ab initio* electronic calculations and not on major simplifying assumptions nor empirical models; and, although much more computer intensive, they give a variety of other useful information, such as validity of the truncation of shells, which determine the applicability of the Hamada *et al* approach.

5. Conclusion

We have presented a formalism for the study of atomic short-range order and the dependence of magnetic properties upon the local chemical environment in ferromagnetic alloys. We have illustrated the approach by presenting details of calculation of Cr–Fe and Fe–V alloys. In the latter case, we have used the moment–compositional response functions to model roughly the magnetic structure of the FeV CMS.

We reiterate that the mean field response of any quantity related to the Green function may be derived via the KKR–CPA. We have only presented results on the environmental response of the moments and outlined the approach for the hyperfine fields. Whereas the thermodynamic response functions give information on bulk phase changes, the 'local' response functions give information on the effects of changes in the local chemical environment. The correlations involved can be investigated and, as a result, the effects of alloying on various properties can be understood on a microscopic basis. It is envisaged that such calculations will aid in the interpretation of the experimental results on various alloys and CMSs and guide researchers in the creation of layered structures with specific properties.

In the future, we plan investigations of ternary alloys with the above theory. Besides helping understand the phase diagrams of such alloys, there come to mind several intriguing possibilities, such as (1) determination of HFF changes of ^{57}Fe impurities in binary alloys, which may be used for characterization purposes; (2) allowing one component of the alloy to be vacancy and thereby studying the effects of a vacancy order/disorder; (3) investigating

qualitatively poisoning effects at metallic interfaces, such as occurs with sulphur on iron; (4) predicting magnetic behaviour for multilayers created from two different alloys, for example, FeMn/NiFe CMSs which exhibit high coercivity due to magnetic wetting.

Acknowledgments

We thank Dr Joe Cable for making his unpublished neutron scattering data available to us. The work was supported in part by the EPSRC in the UK, and by the US Department of Energy, Office of Basic Energy Sciences, Division of Materials Science through a New Initiative Grant under contract No DE-AC04-94AL85000 with Sandia. Also, DDJ acknowledges support from an NRC–NRL research associateship and computational support through the Pittsburgh Supercomputer Centre when this work was first initiated.

Appendix A

All the quantities in equations (22), (23) and (24) are defined analogously to those in the appendices of [19]. The main difference is that the spin indices now refer to the components of the spin polarized electronic quantities. All notation is the same as in [7, 8, 9, 19, 20].

The components of the response of the CPA medium are

$$\lambda^{P}_{L_1\times L_2}(q) = \sum_{L_3\times L_4} \left[I_{L_1\times L_2,L_3\times L_4}(q)\right]^{-1} \zeta^{P}_{L_3\times L_4} \tag{A1}$$

$$\lambda^{c(\alpha),\rho,n}_{\mathrm{conc},L_1\times L_2}(q) = \sum_{L_3\times L_4} \left[I_{L_1\times L_2,L_3\times L_4}(q)\right]^{-1} \zeta^{c(\alpha),\rho,n}_{\mathrm{conc},L_3\times L_4} \tag{A2}$$

$$\lambda^{c(\alpha),\mu}_{\mathrm{conc},L_1\times L_2}(q) = \sum_{L_3\times L_4} \left[I_{L_1\times L_2,L_3\times L_4}(q)\right]^{-1} \zeta^{c(\alpha),\mu}_{\mathrm{conc},L_3\times L_4} \tag{A3}$$

where $\alpha = \mathrm{A}, \mathrm{B}$. The normalization integral, $I_{L_1\times L_2}(q)$, which describes the full response of the CPA medium has the form of a Bethe–Salpeter equation given by

$$\begin{aligned} I_{L_1\times L_2;L_3\times L_4}(q) = \Big\{ & c\left[\left(D^{\mathrm{A},\uparrow}_{L_1L_3} D^{\mathrm{A},\uparrow}_{L_4L_2} + D^{\mathrm{A},\downarrow}_{L_1L_3} D^{\mathrm{A},\downarrow}_{L_4L_2}\right) - \left(X^{\mathrm{A},\uparrow}_{L_1L_3} X^{\mathrm{A},\uparrow}_{L_4L_2} + X^{\mathrm{A},\downarrow}_{L_1L_3} X^{\mathrm{A},\downarrow}_{L_4L_2}\right)\right] \\ & +(1-c)\left[\left(D^{\mathrm{B},\uparrow}_{L_1L_3} D^{\mathrm{B},\uparrow}_{L_4L_2} + D^{\mathrm{B},\downarrow}_{L_1L_3} D^{\mathrm{B},\downarrow}_{L_4L_2}\right) - \left(X^{\mathrm{B},\uparrow}_{L_1L_3} X^{\mathrm{B},\uparrow}_{L_4L_2} + X^{\mathrm{B},\downarrow}_{L_1L_3} X^{\mathrm{B},\downarrow}_{L_4L_2}\right)\right]\Big\} \\ & \times T_{L_1\times L_3,L_4\times L_2}(q) \end{aligned} \tag{A4}$$

where $X^{\alpha,\uparrow(\downarrow)} = [(t^{-1}_{\alpha,i\uparrow(\downarrow)} - t^{-1}_{\mathrm{c},ii})^{-1} + \tau^{C,ii}]^{-1}$ with the angular momentum indices suppressed, and $D^{\alpha,\uparrow(\downarrow)}$ is defined as $[\mathbf{1} + (t^{-1}_{\alpha,\uparrow(\downarrow)} - t^{-1}_{\mathrm{c}}\mathbf{1})\tau^{C,00}\mathbf{1}]^{-1}$, $\alpha = \mathrm{A}, \mathrm{B}$. $t_{\mathrm{A(B)},\uparrow(\downarrow)}$ are the scattering t matrices for the spin up and spin down components of the spin polarized electronic structure; t_{c} and $\tau^{C,00}$ are, respectively, the t matrix and the diagonal component of the scattering path operator, τ^{ij}, for the CPA effective medium. The most important quantity to evaluate in the above expressions is

$$R_{L_1\times L_2,L_3\times L_4}(q) = \Omega^{-1}_{\mathrm{BZ}} \int \mathrm{d}k\, \tau^{c,0}_{L_1L_3}(k)\tau^{c,0}_{L_4L_2}(k+q) \tag{A5}$$

$$T_{L_1\times L_2,L_3\times L_4}(q) = R_{L_1\times L_2,L_3\times L_4}(q) - \tau^{c,00}_{0,L_1L_3}\tau^{c,00}_{0,L_4L_2} \tag{A6}$$

which is the lattice Fourier transform of $\tau^{c,ij}\tau^{c,ji}$ and Ω_{BZ} is the volume of the Brillouin zone.

We now provide detailed expressions for quantities specified in section 2. These are quantities involving single-site scattering terms and three integrals over the unit cell

(although these are replaced by the Wigner–Seitz sphere in the calculations),

$$F^{\alpha,n}_{\uparrow(\downarrow)LL'} = -\int \mathrm{d}r_i\, Z^{\alpha}_{\uparrow(\downarrow)L}(r_i) Z^{\alpha}_{\uparrow(\downarrow)L'}(r_i) f_n(r_i)/u_1 \tag{A7}$$

$$U^{\alpha\mu}_{\uparrow(\downarrow)LL'} = -\int \mathrm{d}r_i\, Z^{\alpha}_{\uparrow(\downarrow)L}(r_i) \left[\frac{\mathrm{d}v_{\mathrm{xc}}(r_i)}{\mathrm{d}\mu_\alpha} + (-)\frac{\mathrm{d}v_{\mathrm{xc}}(r_i)}{\mathrm{d}\mu_\alpha}\right] f^{m}_{\alpha\uparrow(\downarrow)}(r_i) Z^{\alpha}_{\uparrow(\downarrow)L'}(r_i) \tag{A8}$$

$$\begin{aligned} U^{\alpha\rho,n}_{\uparrow(\downarrow)LL'} = -\int \mathrm{d}r_i\, Z^{\alpha}_{\uparrow(\downarrow)L}(r_i) \Bigg[& \int \mathrm{d}r'_i \frac{f_n(r'_i)}{|r_i - r'_i|} \\ & + \left(\frac{\mathrm{d}v_{\mathrm{xc}}(r_i)}{\mathrm{d}\rho_\alpha} + (-)\frac{\mathrm{d}v_{\mathrm{xc}}(r_i)}{\mathrm{d}\rho_\alpha}\right) f_n(r_i)\Bigg] Z^{\alpha}_{\uparrow(\downarrow)L'}(r_i) \end{aligned} \tag{A9}$$

$$\begin{aligned} \zeta^{P}_{L_1\times L_2} = \sum_{L_3,L_4} \Big[& c\left(D^{\mathrm{A},\uparrow}_{L_1L_3} F^{\mathrm{A},1}_{\uparrow L_3,L_4} D^{\mathrm{A},\uparrow}_{L_4L_2} + D^{\mathrm{A},\downarrow}_{L_1L_3} F^{\mathrm{A},1}_{\downarrow L_3,L_4} D^{\mathrm{A},\downarrow}_{L_4L_2}\right) \\ & + (1-c)\left(D^{\mathrm{B},\uparrow}_{L_1L_3} F^{\mathrm{B},1}_{\uparrow L_3,L_4} D^{\mathrm{B},\uparrow}_{L_4L_2} + D^{\mathrm{B},\downarrow}_{L_1L_3} F^{\mathrm{B},1}_{\downarrow L_3,L_4} D^{\mathrm{B},\downarrow}_{L_4L_2}\right)\Big] \end{aligned} \tag{A10}$$

$$\zeta^{c}_{L_1\times L_2} = X^{\mathrm{A},\uparrow}_{L_1L_2} + X^{\mathrm{A},\downarrow}_{L_1L_2} - X^{\mathrm{B},\uparrow}_{L_1L_2} - X^{\mathrm{B},\downarrow}_{L_1L_2} \tag{A11}$$

$$\zeta^{\alpha,\rho,n}_{\mathrm{conc},L_1\times L_2} = c_\alpha \sum_{L_3,L_4} \left[D^{\alpha,\uparrow}_{L_1L_3} U^{\alpha,\rho,n}_{\uparrow L_3,L_4} D^{\alpha,\uparrow}_{L_4L_2} + D^{\alpha,\downarrow}_{L_1L_3} U^{\alpha,\rho,n}_{\downarrow L_3,L_4} D^{\alpha,\downarrow}_{L_4L_2}\right] \tag{A12}$$

$$\zeta^{\alpha,\mu}_{\mathrm{conc},L_1\times L_2} = c_\alpha \sum_{L_3,L_4} \left[D^{\alpha,\uparrow}_{L_1L_3} U^{\alpha,\mu}_{\uparrow L_3,L_4} D^{\alpha,\uparrow}_{L_4L_2} + D^{\alpha,\downarrow}_{L_1L_3} U^{\alpha,\mu}_{\downarrow L_3,L_4} D^{\alpha,\downarrow}_{L_4L_2}\right] \tag{A13}$$

where $c_{\mathrm{A}} = c$ and $c_{\mathrm{B}} = 1 - c$. We can now spell out explicitly the key terms. Firstly, part of the chemical interchange energy

$$\begin{aligned} S^{cc}(q) = \frac{1}{\pi}\mathrm{Im}\int \mathrm{d}\epsilon\, f(\epsilon-\mu) \sum_{LL'} \left((D^{\mathrm{A},\uparrow} + D^{\mathrm{A},\downarrow} - D^{\mathrm{B},\uparrow} - D^{\mathrm{B},\downarrow})(\tau_0^{c,00})^{-1}\right)_{LL'} \\ \times \sum_{L_1\times L_2} T_{L\times L',L_1\times L_2}(q) \lambda^{c}_{\mathrm{conc},L_1\times L_2} \end{aligned} \tag{A14}$$

is the entire contribution when 'band-energy' effects only are considered, i.e., we ignore all charge rearrangement effects. It is the generalization to a paramagnetic alloy of the direct correlation function of Gyorffy and Stocks who considered Fermi surface and band filling (or *e/a*) effects only. The remaining terms can be expressed in a similar way.

$$\begin{aligned} S^{c\rho,n}_{\alpha}(q) = -\frac{1}{\pi}\mathrm{Im}\int \mathrm{d}\epsilon\, f(\epsilon-\mu) \sum_{LL'} \left((D^{\mathrm{A},\uparrow} + D^{\mathrm{A},\downarrow} - D^{\mathrm{B},\uparrow} - D^{\mathrm{B},\downarrow})(\tau_0^{c,00})^{-1}\right)_{LL'} \\ \times \sum_{L_1\times L_2} T_{L\times L',L_1\times L_2}(q) \lambda^{\alpha,\rho,n}_{\mathrm{conc},L_1\times L_2} \end{aligned} \tag{A15}$$

$$\begin{aligned} S^{c\mu,n}_{\alpha}(q) = -\frac{1}{\pi}\mathrm{Im}\int \mathrm{d}\epsilon\, f(\epsilon-\mu) \sum_{LL'} \left((D^{\mathrm{A},\uparrow} + D^{\mathrm{A},\downarrow} - D^{\mathrm{B},\uparrow} - D^{\mathrm{B},\downarrow})(\tau_0^{c,00})^{-1}\right)_{LL'} \\ \times \sum_{L_1\times L_2} T_{L\times L',L_1\times L_2}(q) \lambda^{\alpha,\mu,n}_{\mathrm{conc},L_1\times L_2} \end{aligned} \tag{A16}$$

$$\begin{aligned} S^{cP}(q) = -\frac{1}{\pi}\mathrm{Im}\int \mathrm{d}\epsilon\, f(\epsilon-\mu) \sum_{LL'} \left((D^{\mathrm{A},\uparrow} + D^{\mathrm{A},\downarrow} - D^{\mathrm{B},\uparrow} - D^{\mathrm{B},\downarrow})(\tau_0^{c,00})^{-1}\right)_{LL'} \\ \times \sum_{L_1\times L_2} T_{L\times L',L_1\times L_2}(q) \lambda^{P}_{L_1\times L_2} \end{aligned} \tag{A17}$$

$$\epsilon_{\alpha}^{\rho c;n'}(q) = -\frac{1}{\pi}\mathrm{Im}\int \mathrm{d}\epsilon\, f(\epsilon-\mu)\sum_{LL'}\left(F_{\uparrow}^{\alpha,n'}D^{\alpha,\uparrow}D^{\alpha,\uparrow}+F_{\downarrow}^{\alpha,n'}D^{\alpha,\downarrow}D^{\alpha,\downarrow}\right)_{LL'} \times \sum_{L_1\times L_2} T_{L\times L',L_1\times L_2}(q)\lambda^{c}_{\mathrm{conc},L_1\times L_2} \tag{A18}$$

$$\epsilon_{\alpha}^{\rho P;n'}(q) = -\frac{1}{\pi}\mathrm{Im}\int \mathrm{d}\epsilon\, f(\epsilon-\mu)\sum_{LL'}u_1\left(F_{\uparrow}^{\alpha,n'}D^{\alpha,\uparrow}D^{\alpha,\uparrow}+F_{\downarrow}^{\alpha,n'}D^{\alpha,\downarrow}D^{\alpha,\downarrow}\right)_{LL'} \times \sum_{L_1\times L_2} T_{L\times L',L_1\times L_2}(q)\lambda^{P}_{L_1\times L_2}+\frac{1}{\pi}\mathrm{Im}\int \mathrm{d}\epsilon\, f(\epsilon-\mu)\int \mathrm{d}r_i\, f_{n'}(r_i) \times \int \mathrm{d}r_i'\left(G^{\alpha,\uparrow}(r_i,r_i')G^{\alpha,\uparrow}(r_i',r_i)+G^{\alpha,\downarrow}(r_i,r_i')G^{\alpha,\downarrow}(r_i',r_i)\right) \tag{A19}$$

$$\epsilon_{\alpha\beta}^{\rho\rho;n'n}(q) = -\frac{1}{\pi}\mathrm{Im}\int \mathrm{d}\epsilon\, f(\epsilon-\mu)\sum_{LL'}\left(F_{\uparrow}^{\alpha,n'}D^{\alpha,\uparrow}D^{\alpha,\uparrow}+F_{\downarrow}^{\alpha,n'}D^{\alpha,\downarrow}D^{\alpha,\downarrow}\right)_{LL'} \times \sum_{L_1\times L_2} T_{L\times L',L_1\times L_2}(q)\lambda^{\beta,\rho,n}_{\mathrm{conc},L_1\times L_2} -\delta_{\alpha\beta}\frac{1}{\pi}\mathrm{Im}\int \mathrm{d}\epsilon\, f(\epsilon-\mu)\int \mathrm{d}r_i\, f_{n'}(r_i)\int \mathrm{d}r_i'\left(G^{\beta,\uparrow}(r_i,r_i')+G^{\beta,\downarrow}(r_i,r_i')\right) \times \int \mathrm{d}r_i^*\left[\frac{f_n(r_i^*)}{|r_i'-r_i^*|}+\frac{\mathrm{d}v_{\mathrm{xc}}}{d\rho^{\beta}(r_i')}f_n(r_i')\right]\left(G^{\beta,\uparrow}(r_i',r_i)+G^{\beta,\downarrow}(r_i',r_i)\right) \tag{A20}$$

$$\epsilon_{\alpha\beta}^{\rho\mu;n'}(q) = -\frac{1}{\pi}\mathrm{Im}\int \mathrm{d}\epsilon\, f(\epsilon-\mu)\sum_{LL'}u_1\left(F_{\uparrow}^{\alpha,n'}D^{\alpha,\uparrow}D^{\alpha,\uparrow}-F_{\downarrow}^{\alpha,n'}D^{\alpha,\downarrow}D^{\alpha,\downarrow}\right)_{LL'} \times \sum_{L_1\times L_2} T_{L\times L',L_1\times L_2}(q)\lambda^{\beta,\rho,1}_{\mathrm{conc},L_1\times L_2} -\delta_{\alpha\beta}\frac{1}{\pi}\mathrm{Im}\int \mathrm{d}\epsilon\, f(\epsilon-\mu)\int \mathrm{d}r_i\, f_{n'}(r_i)\int \mathrm{d}r_i'\left(G^{\beta,\uparrow}(r_i,r_i')-G^{\beta,\downarrow}(r_i,r_i')\right) \times \int \mathrm{d}r_i^*\left[\frac{f_1(r_i^*)}{|r_i'-r_i^*|}+\frac{\mathrm{d}v_{\mathrm{xc}}}{\mathrm{d}\rho^{\beta}(r_i')}f_1(r_i')\right]\left(G^{\beta,\uparrow}(r_i',r_i)-G^{\beta,\downarrow}(r_i',r_i)\right) \tag{A21}$$

$$\chi_{\alpha}^{\mu c}(q) = -\frac{1}{\pi}\mathrm{Im}\int \mathrm{d}\epsilon\, f(\epsilon-\mu)\sum_{LL'}u_1\left(F_{\uparrow}^{\alpha,1}D^{\alpha,\uparrow}D^{\alpha,\uparrow}-F_{\downarrow}^{\alpha,1}D^{\alpha,\downarrow}D^{\alpha,\downarrow}\right)_{LL'} \times \sum_{L_1\times L_2} T_{L\times L',L_1\times L_2}(q)\lambda^{c}_{\mathrm{conc},L_1\times L_2} \tag{A22}$$

$$\chi_{\alpha}^{\mu P}(q) = -\frac{1}{\pi}\mathrm{Im}\int \mathrm{d}\epsilon\, f(\epsilon-\mu)\sum_{LL'}u_1\left(F_{\uparrow}^{\alpha,1}D^{\alpha,\uparrow}D^{\alpha,\uparrow}-F_{\downarrow}^{\alpha,1}D^{\alpha,\downarrow}D^{\alpha,\downarrow}\right)_{LL'} \times \sum_{L_1\times L_2} T_{L\times L',L_1\times L_2}(q)\lambda^{P}_{L_1\times L_2}+\frac{1}{\pi}\mathrm{Im}\int \mathrm{d}\epsilon\, f(\epsilon-\mu)\int \mathrm{d}r_i\, f_1(r_i) \times \int \mathrm{d}r_i'\left(G^{\alpha,\uparrow}(r_i,r_i')G^{\alpha,\uparrow}(r_i',r_i)-G^{\alpha,\downarrow}(r_i,r_i')G^{\alpha,\downarrow}(r_i',r_i)\right) \tag{A23}$$

$$\chi_{\alpha\beta}^{\mu\rho;n'}(q) = -\frac{1}{\pi}\mathrm{Im}\int \mathrm{d}\epsilon\, f(\epsilon-\mu)\sum_{LL'}u_1\left(F_{\uparrow}^{\alpha,n'}D^{\alpha,\uparrow}D^{\alpha,\uparrow}+F_{\downarrow}^{\alpha,n'}D^{\alpha,\downarrow}D^{\alpha,\downarrow}\right)_{LL'}$$

$$\times \sum_{L_1\times L_2} T_{L\times L',L_1\times L_2}(q)\lambda^{\beta,\mu,1}_{\mathrm{conc},L_1\times L_2}$$
$$-\delta_{\alpha\beta}\frac{1}{\pi}\mathrm{Im}\int \mathrm{d}\epsilon\, f(\epsilon-\mu)\int \mathrm{d}r_i\, f_{n'}(r_i)\int \mathrm{d}r_i'\left(G^{\beta,\uparrow}(r_i,r_i')+G^{\beta,\downarrow}(r_i,r_i')\right)$$
$$\times\int \mathrm{d}r_i^*\left[\frac{f_1(r_i^*)}{|r_i'-r_i^*|}+\frac{\mathrm{d}v_{\mathrm{xc}}}{\mathrm{d}\rho^\beta(r_i')}f_1(r_i')\right]\left(G^{\beta,\uparrow}(r_i',r_i)+G^{\beta,\downarrow}(r_i',r_i)\right) \tag{A24}$$

$$\chi^{\mu\mu}_{\alpha\beta}(q)=-\frac{1}{\pi}\mathrm{Im}\int \mathrm{d}\epsilon\, f(\epsilon-\mu)\sum_{LL'}u_1\left(F^{\alpha,1}_{\uparrow}D^{\alpha,\uparrow}D^{\alpha,\uparrow}-F^{\alpha,1}_{\downarrow}D^{\alpha,\downarrow}D^{\alpha,\downarrow}\right)_{LL'}$$
$$\times \sum_{L_1\times L_2} T_{L\times L',L_1\times L_2}(q)\lambda^{\beta,\mu,1}_{\mathrm{conc},L_1\times L_2}$$
$$-\delta_{\alpha\beta}\frac{1}{\pi}\mathrm{Im}\int \mathrm{d}\epsilon\, f(\epsilon-\mu)\int \mathrm{d}r_i\, f_1(r_i)\int \mathrm{d}r_i'\left(G^{\beta,\uparrow}(r_i,r_i')-G^{\beta,\downarrow}(r_i,r_i')\right)$$
$$\times\int \mathrm{d}r_i^*\left[\frac{f_1(r_i^*)}{|r_i'-r_i^*|}+\frac{\mathrm{d}v_{\mathrm{xc}}}{\mathrm{d}\rho^\beta(r_i')}f_1(r_i')\right]\left(G^{\beta,\uparrow}(r_i',r_i)-G^{\beta,\downarrow}(r_i',r_i)\right). \tag{A25}$$

Appendix B

The $2n_f+2$ (n_f is the total number of basis functions) quantities that define equation (31), namely $\gamma^n_{\mathrm{A(B)c}}(q)$, $\gamma^m_{\mathrm{A(B)}}(q)$, $\kappa^n_{\mathrm{A(B)c}}(q)$ and $\kappa^m_{\mathrm{A(B)}}(q)$, are given by

$$\begin{bmatrix}\gamma^1_{\mathrm{Ac}}\\ \vdots\\ \gamma^{n_f}_{\mathrm{Ac}}\\ \gamma^1_{\mathrm{Bc}}\\ \vdots\\ \gamma^{n_f}_{\mathrm{Bc}}\\ \gamma^m_{\mathrm{A}}\\ \gamma^m_{\mathrm{B}}\end{bmatrix}=\mathbf{M}\begin{bmatrix}\epsilon^{\rho c;1}_{\mathrm{A}}(q)\\ \vdots\\ \epsilon^{\rho c;n_f}_{\mathrm{A}}(q)\\ \epsilon^{\rho c;1}_{\mathrm{B}}(q)\\ \vdots\\ \epsilon^{\rho c;n_f}_{\mathrm{B}}(q)\\ \chi^{\mu c}_{\mathrm{A}}(q)\\ \chi^{\mu c}_{\mathrm{B}}(q)\end{bmatrix}\qquad\begin{bmatrix}\kappa^1_{\mathrm{Ac}}(q)\\ \vdots\\ \kappa^{n_f}_{\mathrm{Ac}}(q)\\ \kappa^1_{\mathrm{Bc}}(q)\\ \vdots\\ \kappa^{n_f}_{\mathrm{Bc}}(q)\\ \kappa^m_{\mathrm{A}}(q)\\ \kappa^m_{\mathrm{B}}(q)\end{bmatrix}=-\mathbf{M}\begin{bmatrix}\epsilon^{\rho P;1}_{\mathrm{A}}(q)\\ \vdots\\ \epsilon^{\rho P;n_f}_{\mathrm{A}}(q)\\ \epsilon^{\rho P;1}_{\mathrm{B}}(q)\\ \vdots\\ \epsilon^{\rho P;n_f}_{\mathrm{B}}(q)\\ \chi^{\mu P}_{\mathrm{A}}(q)\\ \chi^{\mu P}_{\mathrm{B}}(q)\end{bmatrix}.$$

For brevity, the $(2n_f+2)\times(2n_f+2)$ matrix $\mathbf{M}$ can be expressed as

$$\mathbf{M}=\begin{bmatrix}\delta_{nn'}-\epsilon^{\rho\rho;nn'}_{\mathrm{A,A}}(q) & -\epsilon^{\rho\rho;nn'}_{\mathrm{B,A}}(q) & -\epsilon^{\rho\mu;n'}_{\mathrm{A,A}}(q) & -\epsilon^{\rho\mu;n'}_{\mathrm{B,A}}(q)\\ -\epsilon^{\rho\rho;nn'}_{\mathrm{A,B}}(q) & \delta_{nn'}-\epsilon^{\rho\rho;nn'}_{\mathrm{B,B}}(q) & -\epsilon^{\rho\mu;n'}_{\mathrm{A,B}}(q) & -\epsilon^{\rho\mu;n'}_{\mathrm{B,B}}(q)\\ -u_1\chi^{\mu\rho;n'}_{\mathrm{A,A}}(q) & -u_1\chi^{\mu\rho;n'}_{\mathrm{B,A}}(q) & 1-\chi^{\mu\mu}_{\mathrm{A,A}}(q) & -\chi^{\mu\mu}_{\mathrm{B,A}}(q)\\ -u_1\chi^{\mu\rho;n'}_{\mathrm{A,B}}(q) & -u_1\chi^{\mu\rho;n'}_{\mathrm{B,B}}(q) & -\chi^{\mu\mu}_{\mathrm{A,B}}(q) & 1-\chi^{\mu\mu}_{\mathrm{B,B}}(q)\end{bmatrix}^{-1}$$

where the quantities in the matrix have been defined in appendix A, and $n, n'=1, n_f$.

References

[1] Staunton J B *et al* 1989 *Alloy Phase Stability (NATO ASI Series E163)* ed G M Stocks and A Gonis (Dordrecht: Kluwer) pp 469–507

[2] Staunton J B, Johnson D D and Gyorffy B L 1987 *J. Appl. Phys.* **61** 3693
Staunton J B, Johnson D D and Pinski F J 1990 *Phys. Rev. Lett.* **65** 1259

Staunton J B, Johnson D D, Gyorffy B L and Walden C 1990 *Phil. Mag.* B **61** 773
[3] Jaggi N K, Schwartz L H, Wong H K and Ketterson J B 1985 *J. Magn. Magn. Mater* **49** 1
[4] Hosoito N, Kawaguchi K, Shinjo T, Takada T and Endoh T 1984 *J. Phys. Soc. Japan* **53** 2659
[5] Hamada N, Terakura K and Yanase A 1984 *J. Phys. F: Met. Phys.* **14** 2374
Hamada N and Miwa H 1978 *Prog. Theor. Phys.* **59** 1045
[6] Vega A, Balbás L C, Nait-Laziz H and Demangeat C 1993 *Phys. Rev.* B **48** 985
[7] Staunton J B, Johnson D D and Pinski F J 1994 *Phys. Rev.* B **50** 1450
[8] Johnson D D, Staunton J B and Pinski F J 1994 *Phys. Rev.* B **50** 1473
[9] Ling M F, Staunton J B and Johnson D D 1994 *Europhys. Lett.* **25** 631
[10] Gyorffy B L, Pindor A J, Staunton J B, Stocks G M and Winter H 1985 *J. Phys. F: Met. Phys.* **15** 1337
[11] Pindor A J, Staunton J B, Stocks G M and Winter H 1983 *J. Phys. F: Met. Phys.* **13** 979
[12] Staunton J B, Gyorffy B L, Pindor A J, Stocks G M and Winter H 1985 *J. Phys. F: Met. Phys.* **15** 1387
[13] Brout R and Thomas H 1967 *Physica* **3** 317
[14] Staunton J B and Gyorffy B L 1992 *Phys. Rev. Lett.* **69** 371
[15] Mirebeau I, Parette G and Cable J W 1987 *J. Phys. F: Met. Phys.* **17** 191
[16] Medina R A and Cable J W 1977 *Phys. Rev.* **15** 1539
Cable J W and Medina R A 1976 *Phys. Rev.* B **13** 4868
[17] Marshall W 1968 *J. Phys. C: Solid State Phys.* **1** 88
[18] Hicks T J 1968 *J. Phys. C: Solid State Phys.* **10** 879
[19] Ling M F, Staunton J B and Johnson D D 1994 *J. Phys.: Condens. Matter* **6** 5981
[20] Ling M F, Staunton J B and Johnson D D 1994 *J. Phys.: Condens. Matter* **6** 6001
[21] Stocks G M and Winter H 1982 *Z. Phys.* B **46** 95
[22] Johnson D D *et al* 1986 *Phys. Rev. Lett.* **56** 2088; 1990 *Phys. Rev.* B **41** 9701
[23] Wohlfarth E P 1953 *Rev. Mod. Phys.* **25** 211
[24] Gunnarsson O 1976 *J. Phys. F: Met. Phys.* **6** 587
[25] Johnson D D, Pinski F J and Stocks G M 1985 *J. Appl. Phys.* **57** 3018
[26] Gyorffy B L and Stocks G M 1983 *Phys. Rev. Lett.* **50** 374
[27] Khachaturyan A G 1983 *Theory of Structural Transformations in Solids* (New York: Wiley) p 39
[28] Althoff J, Johnson D D, Pinski F J and Staunton J B 1995 to be published
[29] Feynman R P 1955 *Phys. Rev.* **97** 660
[30] Staunton J B, Johnson D D and Pinski F J 1990 *Phys. Rev. Lett.* **65** 1259
[31] Ducastelle F 1989 *Alloy Phase Stability (NATO ASI Series E163)* ed G M Stocks and A Gonis (Dordrecht: Kluwer) pp 293–328
[32] Pettifor D G 1978 *Solid State Commun.* **28** 621; 1979 *Phys. Rev. Lett.* **42** 846
[33] Gonis A, Stocks G M, Butler W H and Winter H 1984 *Phys. Rev.* B **29** 555
[34] Malozemoff A P, Williams A R and Moruzzi V L 1984 *Phys. Rev.* B **29** 1620
[35] Cable J W, Child H R and Nakai Y 1990 *Physica* B **156 & 157** 50
[36] Cable J W, Gillon B, Mirebeau I, Parette G and Nakai Y 1990 *35th Annual Conf. on Magnetism and Magnetic Materials (San Diego, CA, 1990)* abstract
[37] Aldred A T 1972 *Int. J. Magn.* **2** 223
[38] Johnson D D, Pinski F J and Staunton J B 1987 *J. Appl. Phys.* **61** 3715
[39] Hennion M 1983 *J. Phys. F: Met. Phys.* **13** 2351
[40] Kakehashi Y 1985 *Phys. Rev.* B **32** 3035
[41] Guenzburger D, Ellis D E and Danon J A 1986 *J. Magn. Magn. Mater* **59** 139
[42] Elzain M E, Ellis D E and Guensburger D 1986 *Phys. Rev.* B **34** 1430
[43] Wong H K, Yang H Q, Hilliard J E and Ketterson J B 1985 *J. Appl. Phys.* **57** 3660
[44] Johnson C E, Redout M S and Cranshaw T E 1963 *Proc. Phys. Soc.* **81** 1079
[45] Erich V 1969 *Z. Phys.* **227** 25
[46] Ebert H, Winter H, Gyorffy B L, Johnson D D and Pinski F J 1987 *Solid State Commun.* **64** 1011; 1987 *J. Phys. F: Met. Phys.* **18** 719
[47] Hamada N, Terakura K and Yasuoka H 1985 *J. Phys. F: Met. Phys.* **15** 835